

Residual Set-up Error for Canine Brain Radiation Therapy

A Thesis Submitted to the College of Graduate and Postdoctoral Studies in Partial
Fulfillment of the Requirements for the Degree of Master of Science
in the Department of Small Animal Clinical Sciences
University of Saskatchewan, Saskatoon

Celina Yukari Morimoto, DVM

PERMISSION TO USE

In presenting this thesis in partial fulfillment of the requirements for a Postgraduate degree from the University of Saskatchewan, I agree that the Libraries of this University may make it freely available for inspection. I further agree that permission for copying of this thesis in any manner, in whole or in part, for scholarly purposes may be granted by the professor who supervised my thesis work, and the College of Graduate and Postdoctoral Studies or, in their absence, by the Head of the Department or the Dean of the College in which my thesis work was done. It is understood that any copying or publication or use of this thesis or parts thereof for financial gain shall not be allowed without my written permission. It is also understood that due recognition shall be given to me and to the University of Saskatchewan in any scholarly use which may be made of any material in my thesis.

Requests for permission to copy or to make other use of material in this thesis in whole or part should be addressed to:

Dean of the College of Graduate and Postdoctoral Studies

University of Saskatchewan

116 Thorvaldson Building, 110 Science Place

Saskatoon, Saskatchewan, S7N 5C9, Canada

Head of Department of Small Animal Clinical Sciences

University of Saskatchewan

52 Campus Drive

Saskatoon, Saskatchewan, S7N 5B4, Canada

ABSTRACT

When targeting a structure in three-dimensional space, the repositioning accuracy of the patient on the treatment table should be consistent among all radiation treatment sessions. Immobilization devices are used to reposition the patients, and imaging systems built into the radiation machine are used to correct the patient's position prior to treatment.

Radiation oncologists usually treat a margin of normal tissue around the tumor called planning target volume (PTV) to account for interfraction (set-up errors) and intrafraction motion (such as motion due to respiration). The size of the PTV margin is an estimate of the targeting accuracy that can be achieved using immobilization devices and image guidance. The PTV margin reported for stereotactic radiation therapy (SRT) and stereotactic radiosurgery (SRS) to treat canine brain tumors ranges from 0-3 millimeters (Kelsey, Gieger, and Nolan 2018; Griffin et al. 2014; Dolera et al. 2017).

An ideal margin would be a narrow margin to minimize the chance of toxicity to the normal brain and wide enough to cover the entire tumor target. The size of the PTV margin also depends on the radiation therapy delivery technique and the fractionation scheme (dose of radiation for each treatment session) planned for determined tumor types and locations.

Accurate patient set-up and adequate PTV margin selection are required to minimize the chance of radiation side effects to the normal tissue surrounding the tumor region and to maximize tumor control. This is particularly relevant for SRS and SRT treatments, as higher doses of radiation are used to treat cancers compared to conventional radiation protocols.

ACKNOWLEDGEMENTS

My interest in Oncology started when I was in my second year of my veterinary studies. Through an exchange undergraduate program funded by Global Affairs Canada – the Emerging Leaders in the Americas Program (ELAP) – I was fortunate to meet Dr. Monique Mayer in 2014, who has encouraged, taught, and supported me so much since then. I would also like to thank the incredible team in Radiation Oncology and Medical Oncology for all the knowledge shared with me. I would like to especially express my gratitude to Rachel Bloomfield, the Radiation Therapy Technologist from the Veterinary Medical Centre, who has dedicated a valuable amount of her time in these research projects, and Dr. Andrew Alexander from the Saskatchewan Cancer Centre, for the valuable advices.

I would like to thank my graduate committee members: Dr. Cheryl Waldner, Dr. Narinder Sidhu, and Dr. Vijayananda Kundapur for their important advices, and for dedicating their time during my MSc program.

The funding support from the WCVM Graduate Education Enhancement Fund was essential for creating this great opportunity to advance my education.

Thank you to my family: Mom, Dad, and my sister Jaque for being supportive, and for understanding my absence during all these years that I have been so far away from home.

TABLE OF CONTENTS

PERMISSION TO USE	i
ABSTRACT.....	ii
ACKNOWLEDGEMENTS	iii
TABLE OF CONTENTS	iv
LIST OF TABLES.....	vi
LIST OF FIGURES	vii
LIST OF ABBREVIATIONS.....	viii
1. CHAPTER ONE: INTRODUCTION	1
1.1. External Radiation Therapy Delivery Techniques	1
1.1.1. Manual dose calculations	1
1.1.2. 3D-conformal radiation therapy.....	2
1.1.3. Intensity-modulated radiation therapy	2
1.2. Fractionation Schemes.....	3
1.2.1. Conventional fractionation	3
1.2.2. Hypofractionation.....	4
1.3. Margin Definitions.....	4
Margin calculation	7
1.4. Patient Repositioning	12
1.4.1. Image guidance	12
1.4.2. Positioning devices.....	16
1.4.3. Positioning techniques.....	19
1.5. Sources of Uncertainties in Patient Repositioning	19
1.5.1. Localization accuracy of CT/CBCT	21
1.5.2. Accuracy of image registration.....	22
1.5.3. Mechanical uncertainties of the equipment.....	22
1.5.4. Dosimetric uncertainties	23
1.5.5. Uncertainties in target delineation.....	24
1.6. Objectives	26
1.7. Student's Contribution to the Manuscripts	26
2. CHAPTER TWO: RESIDUAL SET-UP ERROR IN THE CANINE INTRACRANIAL REGION AFTER MV, KV AND CBCT ONLINE CORRECTION FOR RADIATION THERAPY ..	27
2.1. Abstract.....	27
2.2. Introduction	28

2.3.	Materials and Methods	29
2.3.1.	Subject preparation	29
2.3.2.	Immobilization and reference image acquisition	29
2.3.3.	Quality assurance.....	32
2.3.4.	Test set-ups and image guidance.....	33
2.3.5.	Data collection.....	35
2.3.6.	Statistical analysis	36
2.4.	Results	37
2.4.1.	3D displacement before and after image guidance	37
2.4.2.	3D displacement and the residual set-up error	37
2.4.3.	Interobserver variability.....	38
2.5.	Discussion.....	40
2.6.	Conclusion	44
3.	CHAPTER THREE: RESIDUAL SET-UP ERROR FOR CANINE BRAIN RADIATION THERAPY AFTER MV AND CBCT ONLINE CORRECTION USING A HEAD-REPOSITIONER SYSTEM FOR IMMOBILIZATION.....	47
3.1.	Abstract.....	47
3.2.	Introduction	48
3.3.	Materials and Methods	49
3.3.1.	Subject preparation	49
3.3.2.	Immobilization and reference image acquisition	49
3.3.3.	Quality assurance.....	51
3.3.4.	Test set-ups and image guidance.....	51
3.3.5.	Data collection.....	52
3.3.6.	Statistical analysis	52
3.4.	Results	53
3.4.1.	3D displacement before and after image guidance	53
3.4.2.	Comparison between two different immobilization devices	55
3.5.	Discussion.....	55
3.6.	Conclusions.....	59
4.	CHAPTER FOUR: GENERAL DISCUSSION	61
5.	CHAPTER FIVE: CONCLUSIONS AND FUTURE DIRECTIONS.....	66
	REFERENCES	68

LIST OF TABLES

Table 2.1. Translational and 3D displacements (millimeters) prior to image-guided set-up and after MV-, kV-, and CBCT-image-guided couch corrections in six cadaver dogs (n = 90 set-ups for each condition).....	39
Table 3.1. Translational and 3D displacements (millimeters) prior to image-guided set-up and after MV-, and CBCT-image-guided couch correction in six cadaver dogs (n = 72 set-ups for each condition).....	54
Table 3.2. Comparison between the absolute mean values of the 3D displacement of the VMC device and the HRD and after MV-, and CBCT-image-guided couch shifts.	55

LIST OF FIGURES

Figure 1.1. Representation of an estimated set-up error based on couch shift or image displacement calculations, and the “true” set-up error based on implanted fiducials in the skull for intracranial targets.....	20
Figure 2.1. The VMC device used for immobilizing and repositioning patients with intracranial tumors treated with radiation therapy. A: thermoplastic neck cushion ventral to the head and cervical region (I), thermoplastic bite block (dotted arrow), custom-made maxillary plate (II), carbon fiber board (III), vacuum deformable body cushion (IV). B: thermoplastic head mask (V), CT marker (solid arrow).	30
Figure 2.2. The OBI system (solid arrows) and the gantry (dotted arrow) of a Varian Clinac 21EX 6MV linear accelerator.....	32
Figure 2.3. Image matching for patient position correction. A: a lateral view MV radiograph matched with the reference DRR. B: a lateral view kV radiograph matched with the reference DRR. C: transverse view CBCT image matched with the reference CBCT.	34
Figure 3.1. A: One CT marker on the surface of the Z-plate (asterisk); the head-repositioning device has a full-body wooden board (I), a plastic maxillary plate (II), and a rigid Styrofoam pillow (III). B: the plastic maxillary plate showing the drilled holes that allow the maxillary teeth to protrude through. C: the moldable bite block (arrow).	50
Figure 3.2. CBCT images showing the original acquisition plane (A), sagittal plane reconstruction (B), dorsal plane reconstruction (C). Note that each slice does not display the full anatomy of the skull.....	58
Figure 3.3. MV radiographs showing the dorsoventral (A) and the lateral (B) views displaying the full anatomy of the skull.	58

LIST OF ABBREVIATIONS

2D: two-dimensional

3D: three-dimensional

3D-CRT: three-dimensional conformal radiation therapy

4DOF: four degrees of freedom

6DOF: six degrees of freedom

BED: biologically effective dose

CBCT: cone-beam computed tomography

cm: centimeters

CT: computed tomography

CTV: clinical target volume

DRR: digital reconstructed radiographs

EPID: electronic portal imaging device

GTV: gross tumor volume

HRD: head-repositioning device

ICRU: International Commission on Radiation Units and Measurements

IMRT: intensity-modulated radiation therapy

kV: kilovoltage

kVp: kilovoltage peak

LQ: linear-quadratic

mAs: milliampere-second

mm: millimeters

MR: magnetic resonance

MRI: magnetic resonance imaging

MV: megavoltage

n: sample size

OBI: on-board imaging

PTV: planning target volume

SD: standard deviation

SRS: stereotactic radiosurgery

SRT: stereotactic radiation therapy

VMC: Veterinary Medical Centre

VRTOG: veterinary radiation oncology group

1. CHAPTER ONE: INTRODUCTION

Photons are uncharged particles with zero rest mass. High energy ionizing photons (or X-rays) can be generated by a megavoltage linear accelerator after electrons are accelerated to hit a tungsten target. Photons from a linear accelerator are classified as an indirectly ionizing type of radiation. The photons interact with the electrons in tissues and cells to produce secondary electrons. These secondary electrons cause DNA strand breaks, which can lead to lethal chromosomal aberrations, either directly or indirectly (through reactive oxygen species) (Hall and Giaccia 2012). Both direct and indirect damage to DNA can lead to chromosomal aberrations that kill the tumor cell or impair tumor cell division. The energy absorbed by the tissues is measured in Gray (Gy), which corresponds to Joules per kilogram of tissue.

1.1. External Radiation Therapy Delivery Techniques

1.1.1. Manual dose calculations

The radiation is delivered in an even dose distribution for cubic or rectangular structures (LaRue and Custis 2014), resulting in a predictable uniform dose coverage throughout the target volume using two parallel opposed beams.

For this type of technique, the PTV margins are usually in the order of a few centimeters and it frequently results in adjacent normal tissue acute side effects, such as erythema and desquamation of the skin, mucositis, otitis, conjunctivitis and keratitis, depending on the irradiated site (LaDue and Klein 2001). Manual dose calculation does not utilize a computed tomography (CT) image for radiation treatment planning because it does not require accurate targeting of the tumor as the PTV margin is wider.

1.1.2. 3D-conformal radiation therapy

This delivery technique requires a CT image to generate a treatment plan. Organs and structures are contoured and labeled in the CT images using a treatment planning software. The computer calculates the dose to each structure, creating a dose volume histogram, that provides a quantitative description of the tumor dose and the normal tissues around the radiation treatment field.

As an attempt to reduce adjacent normal tissue toxicities, custom-made blocks or static multileaf collimators are used to shape the beams and avoid irradiation of normal structures outside the beam path (LaRue and Custis 2014). This technique allows better targeting accuracy, but the PTV margins are usually in the order of a few centimeters (AAPM Task Group 101, 2010).

1.1.3. Intensity-modulated radiation therapy

The multileaf collimator moves during the treatment, modulating the intensity of the beams to the tumor, and creating a nonuniform beam fluence (Khan and Gibbons 2014). This process results in a better accurate targeting of the tumor, sparing large volumes of normal tissue from being irradiated. Therefore, it can reduce the severity of both acute and late side effects.

The PTV margins applied when this technique is used can vary from centimeters to millimeters (AAPM Task Group 101, 2010), depending on the fractionation scheme used and whether other types of set-up verification are performed. The types of fractionation schemes are further detailed in Section *1.2 Fractionation Schemes*.

Although reducing patient discomfort, the intensity-modulated radiation therapy (IMRT) delivery technique does not primarily improve survival of cancer patients (LaRue and Custis 2014). However, by minimizing the chance of occurrence of side effects, the dose to the tumor can be increased, presumably leading to an increase in tumor control probability.

1.2. Fractionation Schemes

Different fractionation protocols have been published for both human and veterinary patients. Each “fraction” refers to one treatment session using radiation as a therapeutic modality. Fractionation schemes vary in the dose of radiation per treatment session.

1.2.1. Conventional fractionation

In veterinary medicine, this type of fractionation has been the mainstay type of radiation therapy in the last fifty years. The conventional fractionation scheme allows delivery of dose to treat tumors while sparing the surrounding normal tissue through fractionation and PTV margins are usually larger, in the order of a few centimeters. This is based on the fact that normal cells can better repair radiation damage than tumor cells.

The conventional fractionation schemes consist of a relatively large number of fractions to treat tumors, frequently with a low dose per fraction of 2.7 to 4Gy given 3 to 5 times per week to achieve total doses of 42 to 57Gy (Withrow, Vail, and Page 2013).

1.2.2. Hypofractionation

Hypofractionated radiation treatments are defined as large doses of radiation given once daily or less often, over a shorter period of time compared to conventional fractionation schemes. Among the hypofractionated protocols, SRS (single fraction) and SRT (2 to 5 fractions) use IMRT technique and require high spatial accuracy. Therefore, SRS and SRT protocols spare normal tissue by avoidance (AAPM Task Group 42, 1995), and PTV margins are in the order of a few millimeters.

1.3. Margin Definitions

With smaller margins being used in SRS and SRT treatments, the targeting accuracy must be maximized to ensure adequate tumor coverage, and to avoid causing unacceptable side effects to normal tissues. The organs and the structures must be precisely correlated with the x-ray beam. For this reason, those volumes are contoured with a planning software for radiation therapy.

The International Commission on Radiation Units and Measurements (ICRU) is a group composed of experts in radiation medicine. Their mission is to provide recommendations on radiation-related quantities and units, terminology, measurement procedures, and reference data for professionals involved in the medical radiation specialty. According to ICRU Report 62 (1999), the gross tumor volume (GTV) is an anatomical concept in which the shape, size, and location of the tumor is determined by clinical examination and/or imaging techniques (ICRU Report 62, 1999). An expansion from the GTV, called clinical target volume (CTV), is added based on possible extension of subclinical disease depending on the tumor type. The PTV is included around the CTV

with the goal to achieve full coverage of the prescribed dose to the tumor, accounting for geometrical and some technical uncertainties. Therefore, the PTV takes into consideration the internal margin and the set-up margin. The internal margin accounts for physiologic movements. Lastly, the set-up margin is defined as “*uncertainties in patient positioning and alignment of the therapeutic beams during the treatment planning and through all treatment sessions*” (ICRU Report 91, 2017).

For brain tumors, it is reasonable to consider that the internal margin is very low (ICRU Report 62, 1999) since veterinary patients are usually treated under general anesthesia, which will minimize intrafraction motion. As well, motion due to respiration would be low in a dog that is positioned in an immobilization system that secures the head region. In a study by Dieterich *et al.* (2015), the respiratory motion in canine patients treated with intracranial SRS was measured using cine CT scans (Dieterich *et al.* 2015). The authors reported that less than 5% of the patients had an intrafractional motion of more than 1mm. For this reason, the set-up margin might have a more important contribution for PTV estimation than the internal margin.

Since the publication of ICRU Report 50 (1993), the volume definitions of GTV, CTV, and PTV remained unchanged (ICRU Report 91, 2017). The GTV should be independent of the radiation technique used for treatment (ICRU Report 83, 2010). However, with the new technologies available and used for SRT, the size of the PTV margin can be decreased to a few millimeters (AAPM Task Group 101, 2010). Some examples of those technologies are: three-dimensional imaging for tumor delineation (e.g. CT and MRI), image guidance systems for patient position verification on the radiation

treatment table, the use of customizable immobilization devices, and the use of IMRT technique.

In canine brain meningioma clinical studies, Keyerleber *et al.* (2013) have reported the use of a CTV margin of 3 to 5mm plus a PTV margin of 5mm for 3D-CRT (Keyerleber *et al.* 2013), whereas studies in SRT have reported a CTV margin of 2mm or 0mm, with a PTV margin of 1 to 2mm (Griffin *et al.* 2014), or even zero margins added to the tumor volume (Kelsey, Gieger, and Nolan 2018). All studies reported overall median survival times longer than 17 months (19.2 months (Keyerleber *et al.* 2013), 18.7 months (Griffin *et al.* 2014), 17.3 months (Kelsey, Gieger, and Nolan 2018)).

In a clinical study with 42 canine gliomas treated with fractionated SRT with or without temozolomide chemotherapy, larger margins have been used. The CTV margin included peritumoral edema, and a PTV margin of 3mm was also applied (Dolera *et al.* 2017). Based on the veterinary radiation oncology group (VRTOG) criteria, the authors reported that only one case had grade II neurotoxicity.

An ideal PTV margin would account for all uncertainties involved in treatment planning and delivery which will be discussed later in Section 1.5 *Sources of Uncertainties*. Although the IMRT technique for radiation treatment allows normal tissue sparing, excessively large PTVs would be required in order to ensure 100% tumor coverage (ICRU Report 83, 2010). For this reason, it is acceptable that the PTV margin encompassing normal tissue (such as brain in intracranial tumors irradiation) might have to be compromised to reduce the risk of side effects due to the delivery of SRS or SRT treatments (ICRU Report 83, 2010; ICRU Report 91, 2017).

On the other hand, reducing the PTV size may compromise outcome. A veterinary clinical study has investigated 34 dogs with brain masses treated with low-dose multifractionated (conventional fractionation) radiation therapy based on computer-generated plans (Bley et al. 2005). The study concluded that patients who had a larger PTV/brain volume ratio had a longer survival time.

For intracranial SRS treatments, the CTV can be treated as the GTV, meaning that the CTV may not be contoured as a clinical choice, because targeting all the microscopic disease is not the goal of SRS treatments. Some authors believe that tumor cell death in SRS treatments occur from other mechanisms than just damage of the DNA and this is further discussed in Section 0

New Radiobiology” Hypothesis

. However, even though SRT leads to steep dose gradients around the tumor, there will be a penumbra region outside the GTV that receives a high dose, and this may be sufficient to target the microscopic tumor extension (ICRU Report 91, 2017).

Margin calculation

Numerous margin formulas and other methods to calculate the PTV margin to ensure coverage of the GTV have been studied. The American Association of Physicists in Medicine Radiation Therapy (AAPM) has published a 3D displacement formula based on translational errors in x, y, and z directions (AAPM Task Group 68, 2005). The 3D displacement estimates the error in three-dimensional space and uses the square root of the vectors' square sum, represented by the formula below:

$$\sqrt{x^2 + y^2 + z^2} \dots\dots\dots(1.1)$$

van Herk (2004) has published an extensive review of the different margin formulas. When generating the dataset for a study that reports a formula to estimate margin errors, the number of measurements per patient, and differences between individual patients should be considered in the model to realistically represent the variability of patients (van Herk 2004).

I. van Herk et al. (2000)

$$\text{PTV margin} = 2.5\Sigma + 0.7\sigma' \dots\dots\dots(1.2)$$

Σ = systematic errors

σ' = random errors

Systematic errors are defined by the reproducibility of treatment preparation, because they would affect all treatment fractions in a similar way (van Herk 2004; AAPM Task Group 68 2005). According to the same author, there is a high likelihood that a geographic miss will occur if the systematic patient positioning error is large (van Herk 2004).

Random errors include physiological processes, such as respiration, circulation, peristalsis, degree of filling of anatomical structures, and daily patient set-up differences (AAPM Task Group 68, 2005). Random interfractional positioning errors can be better estimated with larger number of fractions (AAPM Task Group 68, 2005).

Delineation uncertainties (GTV contouring on CT and/or MR images) are essentially systematic errors while set-up errors (daily patient positioning for treatment) are composed of both systematic and random errors (van Herk 2004).

The systematic errors are calculated as the standard deviation of the means of all patients and the random errors are calculated as the root mean square of the all patients' standard deviations. This model estimates the set-up margin based on calculation of systematic and random errors. The margin formula was created to ensure that at least 95% of the prescribed dose to the CTV is delivered to 90% of the patients.

This method has several limitations when applied to SRS and SRT patient margin estimation. Some of the assumptions when this formula is used is that the data are normally distributed, the patient population is homogeneous, and that many fractions are given. The number of fractions directly affects the random errors, in which SRS and SRT protocols would have random errors different from zero. If many fractions are given such as in conventional fractionation scheme, the random error is assumed to be zero as the relative values are smoothed out around the zero coordinate.

Systematic errors were accounted in the formula, and it has been shown to cause more impact than random errors for large number of fractions. This information may not apply for SRS or SRT treatments, as the random error is different from zero. When systematic errors are large, it can shift the whole dose distribution and cause geographical misses (van Herk et al. 2000; van Herk 2004).

II. Lutz *et al.* (1988)

Using the Z score to estimate the cumulative probability in a normal distribution, the authors estimated the margin necessary to encompass the positional accuracy error of radiation treatment delivery to a target localized with CT image guidance (Lutz, Winston, and Malleki 1988). Assuming a normal distribution of the values, the authors used the standard deviation of the mean to estimate the value that would represent the cumulative probability of 90% to estimate that the *“distance error in an individual treatment should be less than 2.4 mm 95% of the time”*.

$$P(x \leq \mu + Z\sigma) \dots\dots\dots(1.3)$$

Where:

P: cumulative probability of 90%

Z: score on the Z-Probability table

μ : mean

σ : standard deviation

For a cumulative probability of 0.90, a corresponding Z score of 1.65 is attributed using the Z-Probability table. Therefore: $P(x \leq \mu + 1.65\sigma)$.

III. AAPM Task Group 68 (2005)

Accuracy is defined as the *“deviation of patient position relative to a reference position at the time of treatment planning”* (AAPM Task Group 68, 2005). Accuracy errors are considered systematic when treatment plans are delivered in a single dose of radiation for a single individual but are stochastic for a group of patients (van Herk et al. 2000). *Precision* is defined as *“how well the position can be determined, i.e., the variability in a set of measurements”* (AAPM Task Group 68, 2005).

The PTV margins used in conventional fractionated therapies, have been decreased in the order of centimeters to millimeters for SRT (AAPM Task Group 101, 2010). This reduction has been based on the assumption of an improvement in targeting accuracy and precision. (AAPM Task Group 68, 2005), due to the development of better immobilization devices and the use of image guidance for patient repositioning.

According to the AAPM Task Group 68, the 95th percentile of the 3D displacement represents the value of the PTV that would be enough to encompass the GTV in 95% of the patient set-ups (AAPM Task Group 68, 2005), and it refers to a margin number generated directly from the experimental model. For this reason, this method does not rely on the assumption that the data follow a normal distribution (AAPM Task Group 68, 2005). Three veterinary studies have also reported the use of the 95th percentile to report margins for intracranial radiation treatments using different positioning devices (Mayer et al. 2010; Hansen et al. 2015; Dieterich et al. 2015).

For conventionally fractionated treatments, a PTV margin based on 5% chance of missing the target could be considered acceptable because 18 or more fractions are delivered to the patient. For this reason, the consequence of a targeting error in one fraction would be relatively smaller in conventional fractionated treatments than SRS or SRT protocols.

When SRS or SRT plans are delivered, a geographic miss could result in catastrophic consequences to the normal tissue, because larger doses per fraction are given. A balance must be determined between the risk of tumor miss and the chance of causing normal tissue toxicity. Higher percentile values than the 95th percentile could be aimed for SRT or SRS treatments, because improvements in image guidance

technologies and the use of more accurate positioning devices may be enough to guarantee small set-up error when the patients are positioned on the radiation treatment table.

1.4. Patient Repositioning

It is essential that the patients are consistently repositioned in a similar way to ensure highly accurate radiation treatment delivery. Patient repositioning techniques, such as image guidance and immobilization devices are used for accurate correlation of the patient to the imaging devices (CT and/or MRI), and to the radiation treatment machine.

1.4.1. Image guidance

Image-guided techniques can be used to achieve a more accurate patient positioning (ICRU Report 83, 2010). They involve using the patient's position from the planning CT scan as a reference, which needs to be repeated for every radiation treatment.

Before each radiation treatment delivery, the patient is positioned using the same immobilization device, and imaging is performed to compare the patient's position with their reference CT image, which shows the position from when the CT scan was acquired to generate the radiation plan. The two sets of images are matched using both automatic software-based registration and also manual registration performed by a radiation therapist or a radiation oncologist.

There are two main types of imaging modalities for patient position verification: planar systems (Electronic Portal Imaging Device and kilovoltage radiographs), and volumetric systems (e.g. cone-beam computed tomography).

I. Planar Systems

For planar pretreatment verification, a digital reconstructed radiograph (DRR) generated from the reference CT image can be verified by matching megavoltage radiographs or kilovoltage radiographs. One potential disadvantage of this type of image guidance is that it only provides two-dimensional information about the patient position.

- Electronic Portal Imaging Device (EPID)

This was the first imaging system available for image guidance in radiation therapy (ICRU Report 91, 2017). It consists of megavoltage (MV) radiographs that use the radiotherapy treatment source (e.g. the gantry of a linear accelerator) to generate high-energy x-rays. MV radiographs result in low contrast images because high energy x-rays are attenuated to a similar degree by bone and soft tissue. Nevertheless, bony anatomy can still be distinguished from soft tissue, but the image contrast is not as high as kilovoltage energy ranges.

- Kilovoltage Radiographs

Kilovoltage (kV) imaging usually consists of two opposed flat panels, orthogonal to the radiation treatment x-ray source. The energy range is much lower than MV energies,

and similar to what it is used for diagnostic x-ray imaging. This technology provides a high contrast between the bones and the soft tissue around them.

Compared to MV port images, kV radiographs expose the patients to lower doses of radiation for set-up correction. However, it is possible to estimate the dose to the patient when EPIDs are acquired, and this dose can be subtracted from the total dose planned for the treatment. Therefore, exposing the patient to higher doses by acquiring MV radiographs should not be a limitation for its use.

II. Volumetric Systems

For three-dimensional verification, the reference CT image acquired for the radiation treatment plan can be matched to a kilovoltage cone-beam computed tomography (CBCT) scan, an in-room mounted CT scanner, an MV fan beam CT, a digital tomosynthesis, a three-dimensional ultrasound, and an in-room mounted MRI (ICRU Report 91, 2017).

The use of the CBCT system has been reported in veterinary patients (Griffin et al. 2014; Dolera et al. 2017; Kelsey, Gieger, and Nolan 2018). This type of image can be generated using the same kV x-ray source as the kV planar radiographs. One of the advantages of using a CBCT scan for patient position correction is that this modality provides spatial information of anatomical structures. For this reason, it is possible to evaluate positional rotations of the patient. One limitation of this method is that the image quality (pixel resolution) can affect the accuracy of patient positioning, because the true patient position may not accurately correlate to the position shown on imaging (Fu et al. 2014).

Careful quality assurance procedures must be performed to ensure adequate spatial correlation between imaging systems and the radiation beam source. This is especially more relevant for kV and CBCT imaging sources, as the x-ray tube is not the same as the radiation machine x-ray source (e.g. the gantry of a linear accelerator).

1.4.2. Positioning devices

Several positioning devices have been evaluated for immobilization of the head in dogs and cats for radiation therapy (Kippenes *et al.* 2000; Rohrer Bley *et al.* 2003; Harmon, Van Ufflen, and LaRue 2009; Kent *et al.* 2009; Charney *et al.* 2009; Kubicek *et al.* 2012; Mayer *et al.* 2010; Hansen *et al.* 2015; Dieterich *et al.* 2015; Nemoto *et al.* 2015).

Kippenes *et al.* (2000) compared three types of positioning devices. Group 1 had a commercial headrest (Silverman supports, Med-Tec, Orange City, IA, USA) and a thermoplastic mask (Uniframe[®] system, Med-Tec, Orange City, IA, USA) secured to a frame, and the system was not indexed (fixed) to the treatment table. Group 2 had a head holder designed at Washington State University and was combined with a ventral neck region support and a dental mold (Polyform[®] splinting material. Smith & Nephew, Germantown, WI, USA). Group 3 had the same head holder and dental mold as Group 2, and a vacuum-locked bag (Vac-lok[™], Med-Tec, Orange City, IA, USA) was added to this system to immobilize the thoracic and cervical regions. The head holder used in Group 2 and Group 3 was indexed to the treatment table. The authors found that Groups 2 and 3 achieved a significantly better repositioning accuracy when compared to Group 1.

Three studies from the University of California have been published in which maxillary plates or bite blocks were not used (Kent *et al.* 2009; Hansen *et al.* 2015; Dieterich *et al.* 2015).

In the first study published, Kent *et al.* (2009) evaluated the accuracy and precision of a positioning device that was not indexed to the treatment table. The device was composed by a thermoplastic mask (Klarity standard U-frame, Klarity Medical &

Equipment (GZ) Co. Ltd., Lan Yu, China) and a customizable head support (MoldCare pillow, Bionix Development Corporation, Toledo, OH, USA) that were secured to a plastic base frame. The mean 3D displacement \pm SD was 2.4 \pm 2.1mm. The authors also calculated the 95th percentile of the 3D displacement, which had the value of 6.4mm.

In a second study, the results from Kent *et al.* (2009) were compared to another positioning device indexed to the treatment table (Hansen et al. 2015). The device had a vacuum-locked bag (SecureVac, Bionix Development Corporation, Toledo, OH, USA), and the same thermoplastic mask and the customizable head support from the previous study. The mean 3D displacement was 1.6mm, and the 95th percentile was 3.6mm.

The third study published from the University of California (Dieterich et al. 2015) consisted on testing a non-indexed immobilization device with a three-piece thermoplastic mask system (Brainlab AG, Feldkirchen, Germany), a vacuum-locked bag, and a head support (Dieterich et al. 2015). The mean 3D displacement reported was 1.9mm, and the 95th percentile was 3.5mm.

Other studies in veterinary medicine have used maxillary plates with or without bite blocks (Rohrer Bley et al. 2003; Harmon, Van Ufflen, and LaRue 2009; Charney et al. 2009; Mayer et al. 2010; Kubicek et al. 2012; Nemoto et al. 2015). Mayer *et al.* (2010) have evaluated the head-repositioning device (HRD) designed by Charney *et al.* (2009). The HRD is a non-indexed immobilization device. The study compared the use of the HRD *versus* patient positioning without the use of an immobilization device, only palpating bony landmarks and using the in-room laser alignment beams (Mayer et al. 2010). The mean 3D displacement and the 95th percentile for the HRD were 0.9mm and 1.9mm, and for the bony palpation method 2.6mm and 4.6mm, respectively. The device designed by

Charney *et al.* (2009) consisted of a non-indexed wooden board that had a maxillary plate to fit a dental mold (VP Mix Putty®, Henry Schein, Melville, NY, USA) with a rigid foam neck support. The maxillary plate that extended from the incisors to the molar teeth had customized holes to allow the dental mold to protrude through the plate.

Another study also reported an improvement in patient positioning when the canines and the fourth premolars were supported by the maxillary plate, compared to the canine teeth alone (Nemoto *et al.* 2015). The maxillary plate had a groove on the top surface, which held the fourth premolar teeth, and the canines had to touch the flat surface of the plate. Based on Mayer *et al.* (2010) and Nemoto *et al.* (2015) studies utilizing maxillary plates that incorporated areas caudal to the fourth maxillary premolar teeth, it is possible that the inclusion of a greater extent could aid in better patient immobilization and repeatability of the position on the treatment table.

Kubicek *et al.* (2012) reported that the use of a vacuum-locked bag (Vac-Lok™ CIVCO, Orange City, IA, USA) with a maxillary support and a bite block (3M-Express STD Putty™ 3M ESPE Dental Products, St. Paul, MN, USA) that is fixed to the treatment table resulted in a statistically better positioning accuracy than the use of the vacuum-locked bag without a bite block.

Overall, immobilization devices with a maxillary plate involving the two canines and both fourth premolar teeth in the bite block, seem to confer a good patient repositioning reproducibility. Indexing the immobilization device to the treatment table seems to provide controversial results regarding the accuracy of patient set-up.

1.4.3. Positioning techniques

When using immobilization devices, the patient's position needs to be correlated to the treatment isocenter. Therefore, additional methods for patient repositioning are used, such as room lasers, and the treatment table index values.

Skin reference marks with a permanent marker or alignment tattoos on the patient can be correlated to the room laser alignment beams. However, dogs and cats' skin are particularly mobile, making this technique unreliable to accurately position the patient on the treatment table. For this reason, the use of room lasers combined with bony landmark palpation were evaluated in a veterinary study (Mayer et al. 2010). Other authors have reported the use of room lasers for alignment with reference marks placed on the positioning devices (Charney et al. 2009; Dieterich et al. 2015).

Table index values can only be used when the positioning device is attached to the table (Kippenes et al. 2000). During the reference patient positioning, the reference table position is recorded and repeated for every treatment set-up.

1.5. Sources of Uncertainties in Patient Repositioning

Estimates of set-up error without image guidance for the canine head have been made using kV radiographs (Harmon, Van Ufflen, and LaRue 2009), MV radiographs (Hansen et al. 2015; Kent et al. 2009) and CT (Dieterich et al. 2015). The kV or MV radiographs were matched to the DRR, while the CT images after repositioning the patient were matched to the reference CT. Those methodologies assumed that image-matched position would be equal to the reference position. However, it is known that the set-up error after image-matching correction can result in residual set-up errors (Meeks et al.

2000; van Herk et al. 2000; Guckenberger et al. 2007; Masi et al. 2008; Dhillon et al. 2017). Some of the reasons for the occurrence of set-up errors are the inability to correct rotations, the couch shift capability of correcting submillimeter differences in translational directions, localization accuracy of the imaging modalities used for image guidance, and isocenter differences within room lasers, on-board imaging (OBI) and the linear accelerator's gantry.

An inherent limitation of clinical studies is that they cannot evaluate the “true” position of the skull in the radiation treatment table because they are usually limited by reporting an estimate of the set-up error by calculating couch shifts or image displacements (Figure 1.1). Those methodologies completely rely on bony anatomy matching. One human phantom study (Chang et al. 2007) and one veterinary study (Mayer et al. 2010) have used fiducial markers embedded inside the skull of the phantom (Brown-Roberts-Wells phantom), or implanted in the surface of live dogs skulls (Suremark 0.2 cm, The Suremark Company, Simi Valley, CA). The fiducials were measured from radiographic orthogonal images to measure the “true” position.

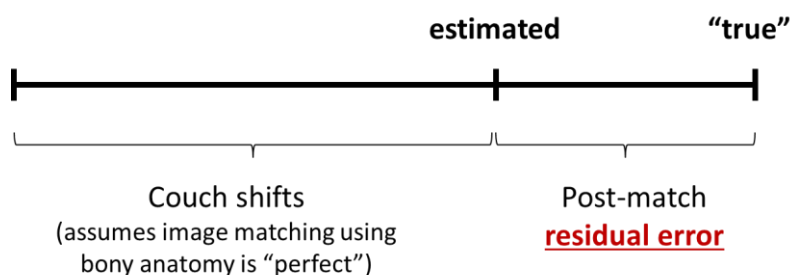


Figure 1.1. Representation of an estimated set-up error based on couch shift or image displacement calculations, and the “true” set-up error based on implanted fiducials in the skull for intracranial targets.

Patient set-up errors have both systematic and random components. The use of an adequate immobilization device combined with image guidance techniques are believed to reduce patient set-up uncertainties. However, to our knowledge, post image guidance set-up errors (residual errors) have not been evaluated in the head region for veterinary patients.

1.5.1. Localization accuracy of CT/CBCT

The accuracy of CBCT image guidance for SRS set-up has been reported (Chang et al. 2007). In that study, a human head phantom containing fiducial markers was repositioned in a stereotactic head frame, and a CBCT of 2mm slice thickness was acquired to calculate the translational corrections to align the fiducial markers with the reference coordinates. Without performing the couch shifts calculated by the CBCT-CT matching, an orthogonal kV radiograph was acquired and compared to the CBCT-based corrections. The mean 3D difference between the CBCT and orthogonal kV radiograph corrections was **1.34mm**.

A CT slice thickness of 2mm introduces an uncertainty in the longitudinal direction of approximately 1mm, which corresponds to half of the slice thickness (Charney et al. 2009). It is possible to reconstruct CT and CBCT scans to 1.0mm slice thickness (Huang et al. 2016). However, Charney *et al.* (2009) have mentioned that using a slice thickness smaller than 2mm would unlikely improve accuracy because there are other uncertainties introduced in patient repositioning, such as CT pixel size resolution and gantry angle precision, among others.

1.5.2. Accuracy of image registration

Image registration or image fusion uncertainties can occur when image guidance is used in radiation therapy. This could possibly result in inaccuracies during treatment due to possible errors that can be introduced when the reference CT and the pretreatment images prior therapy are used for patient repositioning. A human phantom study has found that image registration from a conventional CT scan with a CBCT image can add a mean error of **0.28mm** (Chang et al. 2007).

The ICRU 91 recommends performing automated image registration using software tools followed by manual verification by the radiation therapist (ICRU Report 91, 2017).

1.5.3. Mechanical uncertainties of the equipment

The laser position is considered acceptable if it is within **1mm** from the radiation machine gantry isocenter (ICRU Report 91, 2017).

Two factors can directly influence patient repositioning after image guidance:

I. Couch shift precision

There are commercially available radiation tables that can shift the couch top with 0.1mm increments. The most commonly systems used to treat animals are equipped with couch tops capable of 1mm shifts. In those cases, a translational shift of $\leq 0.5\text{mm}$ cannot be precisely corrected.

Assuming that the use of a couch limited by 1 mm shifts can contribute up to 0.5mm errors in each of the x, y, and z directions, the 3D displacement in this couch system can add up to $\sqrt{(0.5)^2 + (0.5)^2 + (0.5)^2} = \mathbf{0.87mm}$.

II. Correction of rotation

Four degrees of freedom (4DOF) tables can correct all three translational directions (x, y, and z vectors) and yaw rotation. The six degrees of freedom (6DOF) tables can correct the four degrees plus roll and pitch deviations. In theory, a 6DOF table would result in a better repositioning precision. The correction of rotations is even more important for irregularly shaped tumors because uncorrected yaw, pitch, and roll deviations could result in a geographic miss of the target if adequate margins are not added to compensate for them (Peng et al. 2010; Dhillon et al. 2017). When considering the volume of brain tissue and brain tumor volume ratio, intracranial tumors in dogs are proportionally larger than human brain tumors. For this reason, rotation may be even more relevant in veterinary medicine.

Kelsey *et al.* (2018) have reported the outcome for canine meningiomas treated with stereotactic radiosurgery without CTV or PTV expansions, and using a 6DOF couch (Kelsey, Gieger, and Nolan 2018). However, the potential adverse events were similar to a study that reported canine meningioma cases treated with a fractionated SRT protocol using a 4DOF table (Griffin et al. 2014), even though the radiation treatments were planned with similar normal tissue constraint parameters.

1.5.4. Dosimetric uncertainties

Some of the dosimetric uncertainties are related to output factors, dose calculation algorithm uncertainties, and penetration of the beam (ICRU Report 83, 2010; ICRU Report 91, 2017). These factors are not going to be further detailed in this thesis.

1.5.5. Uncertainties in target delineation

Uncertainties in target delineation relate to errors during the radiation planning portion and they contribute to PTV margin selection.

I. Correlation of histopathology and diagnostic imaging

It has been reported that the real tumor extension proven by histopathological evaluation can be different to the tumor area that is visible in CT or MR images (Jansen et al. 2000). One study has found that approximately 35% of untreated glioma patients had tumor cells present outside the hyperintense areas visualized in MR T2-weighted images (Watanabe, Tanaka, and Takeda 1992).

II. Treatment policy, intra- and interobserver variability

The *treatment policy* term is related to each radiation oncologist's decision on treating or not the entire macroscopic and/or microscopic tumor volume (Jansen et al. 2000). Some radiation oncologists include edema as being part of the GTV or CTV, but the amount of edema is partially related to steroid dose and it can be variable (Cattaneo et al. 2005).

Besides differences in treatment policy, the intra- and interobserver delineation uncertainty is another contributor to target delineation uncertainties. The intraobserver variability consists on differences in contouring of the same set of images, made by the

same observer during distinct time frames. The interobserver variability is related to differences in tumor delineation between two or more observers.

In a study by Weltens *et al.* (2001), MR-CT volumes were larger than on CT alone by 10% ($p < 0.01$), but some volumes were delineated on CT and not on MR. For this reason, combination of both modalities is recommended, even though there was no statistical difference in the interobserver variability when CT was used alone or in combination with MR (Weltens *et al.* 2001). Furthermore, the study found maximum variations in the lateral, vertical, and longitudinal directions of 10.7mm, 5.3mm, and 4.4mm, respectively. Using the 3D formula presented previously, these values would correspond to a 3D displacement of **12.7mm**.

III. CT-MR co-registration

It has been shown that combining MR and CT tumor volume information is the best approach to ensure better tumor coverage in radiation therapy (Haken *et al.* 1992).

In veterinary patients, MR images can be used for tumor delineation with or without perfect fusion with CT images (Kelsey, Gieger, and Nolan 2018). When CT and MR images are not co-registered with image fusion, it means that MR images are used to help defining tumor extension by visual comparison of the two image modalities. However, co-registering the MR images without image fusion means that the patient was not in the same position as the planning CT scan. This can contribute to inaccuracy in spatial resolution and errors in tumor delineation (Rosenman 2001). A study by Cattaneo *et al.* (2005) found that the interobserver concordance index for fused CT-MR was

significantly smaller ($p < 0.02$) compared to when visual comparison of CT-MR scans is used (Cattaneo et al. 2005).

1.6. Objectives

To the author's knowledge, there are no studies in the veterinary medicine literature reporting the residual set-up error for radiotherapy patients. Although this error has been previously hypothesized to be in the submillimeter range (Harmon, Van Ufflen, and LaRue 2009; Dieterich et al. 2015), studies in the human medicine have reported that set-up errors remain after couch shift corrections based on image guidance.

1.7. Student's Contribution to the Manuscripts

The student has done a literature review on residual set-up error studies published in human patients, and a literature review on set-up errors for the canine head region.

The selection of the six dog cadavers for this experiment was performed by the student and the supervisor. The implantation of the five fiducial markers in all 12 dogs' skulls was done by the student. The student was responsible for the proper storage of the dogs during the experiments. All 414 set-ups were concomitantly performed by the student and the supervisor.

The student collected all the data on the fiducial markers' positions using the ARIA software (Varian Medical Systems, Palo Alto, CA) and registered the data in a spreadsheet.

Initial drafting of both manuscripts was done by the student. The student and all the co-authors were responsible for revision of the manuscripts.

2. CHAPTER TWO: RESIDUAL SET-UP ERROR IN THE CANINE INTRACRANIAL REGION AFTER MV, KV AND CBCT ONLINE CORRECTION FOR RADIATION THERAPY

This manuscript has been submitted to the Veterinary Radiology & Ultrasound on January 22nd, 2019 and is being evaluated for publication in the current date (Feb 28th, 2019). The copyright of this chapter will belong to the journal it will be published in.

2.1. Abstract

The residual set-up error is not a concept that has been extensively investigated in the veterinary literature. This study aimed to quantify the set-up error that remains after MV-, kV-, and CBCT-image guidance and couch shift corrections are performed for the canine head region radiation therapy. Six dogs were positioned 45 times as for clinical treatment using a vacuum deformable body cushion, a customizable head cushion, a thermoplastic mask, and a maxillary plate with a dental mold. Five lead markers were implanted in the skull of the canine cadavers to measure the residual set-up error using orthogonal kV radiographs. The 95th percentiles of the 3D displacements after online MV, kV, and CBCT-guided correction were 2.8mm, 2.6mm and 3.6mm, respectively, and 4.2mm for the immobilization device without image guidance. In order to avoid important geographical miss, residual set-up errors should be included in the planning target volume margin when stereotactic radiation treatments are planned. Under the conditions of this study, which included a 4 degrees-of-freedom couch with 1mm increment translational move capability, online correction of the canine head region using MV and kV guidance resulted in better accuracy than correction using CBCT guidance.

2.2. Introduction

Image guidance aids in margin reduction to be added around the tumor volume for radiation treatments by increasing targeting accuracy (Dieterich et al. 2015; Hansen et al. 2015; Harmon, Van Ufflen, and LaRue 2009; Kent et al. 2009). Two-dimensional image guidance, such as MV and kV radiographs, or 3D-imaging techniques (i.e. CBCT) can be used for pretreatment patient position verification.

Residual set-up errors are displacements that remain after couch corrections are performed using image-guided techniques. They have been previously hypothesized to be in the submillimeter range (Harmon, Van Ufflen, and LaRue 2009; Dieterich et al. 2015), however errors in the millimeter range have been proved to remain (Meeks et al. 2000; van Herk et al. 2000; Guckenberger et al. 2007; Masi et al. 2008; Dhillon et al. 2017). Residual set-up errors have not been measured in veterinary medicine prior to this work.

The inaccuracies in patient repositioning are related to localization accuracy of the CT scan, accuracy of image registration, mechanical uncertainties of the equipment, variations in patient positioning, and uncertainties in target delineation. If all the possible uncertainties were taken into account to compose a tumor margin, the volume irradiated would likely be so large that an unacceptable risk of normal tissue irradiation could result. On the other hand, insufficient margins could also lead to treatment failure if significant volumes of tumor tissue are not irradiated.

The objective of this study was to measure the residual set-up error after position correction guided by pretreatment MV or kV radiographs, or CBCT scans, using spherical lead markers implanted in the skull of six dog cadavers and a 4DOF couch. Considering

that CBCT allows visualization of both bones and soft tissues in three-dimensional space, the hypotheses were that image guidance would reduce set-up error, and that residual set-up error would be lower after CBCT-based correction than MV- or kV-based correction for the head region.

2.3. Materials and Methods

2.3.1. Subject preparation

Six dog cadavers (median weight 24.3kg, range 21.6-30.6kg) with a mesaticephalic skull conformation were used to simulate canine patients in this study. The University of Saskatchewan's Animal Research Ethics Board (protocol number 20150073).

For each dog, a cutaneous incision of 2.5cm was made, and the musculature was dissected in order to visualize the following regions of the cranial bones: left nasal bone, left cranial zygomatic bone, right temporal bone, right caudal zygomatic bone, and left occipital bone. Using a mechanical drill, the bones were drilled to a depth of approximately 2mm, to fit the 2mm spherical lead markers (Suremark® X-ray labels SL-20, The Suremark Company, Simi Valley, CA). The lead markers were fixed with tissue adhesive (3M Vetbond, 3M Animal Care Products, Saint Paul, MN), and the musculature, subcutaneous tissue, and the skin were also closed using the tissue adhesive.

2.3.2. Immobilization and reference image acquisition

The dogs were immobilized in sternal recumbency using a vacuum deformable body cushion (SecureVac™, Bionix Radiation Therapy, Toldeo, OH), a thermoplastic

neck cushion ventral to the head and cervical region (Klarity™ Moldable AccuCushion, Klarity Medical Products, Newark, OH), a custom-made maxillary plate (6.0 cm width x 9.5 cm height x 17.1cm length) with variable length of maxillary teeth immobilization (incisors to 1st to 4th premolar), thermoplastic bite block (EZ Bolus Thermoplastic Pellets, Klarity Medical Products, Newark, OH) and a thermoplastic head mask dorsal to the head region (Green Profile Frame Extended Head Mask, Klarity Medical Products, Newark, OH). The maxillary plate had three holes of 6mm on its surface that made it possible to fix the thermoplastic bite block. In this system, the thermoplastic head mask was not attached to the maxillary plate. Four screws attached the thermoplastic mask to the carbon fiber board. All the items were attached to a carbon fiber board that was indexed to the treatment table. This immobilization system (VMC device) is the same device used for clinical patients at the Veterinary Medical Centre (VMC), University of Saskatchewan (Figure 2.1).

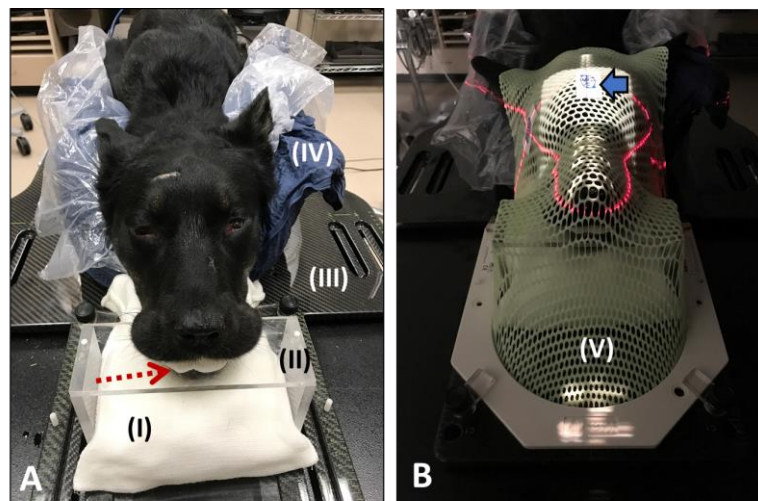


Figure 2.1. The VMC device used for immobilizing and repositioning patients with intracranial tumors treated with radiation therapy. A: thermoplastic neck cushion ventral to the head and cervical region (I), thermoplastic bite block (dotted arrow), custom-made

maxillary plate (II), carbon fiber board (III), vacuum deformable body cushion (IV). B: thermoplastic head mask (V), CT marker (solid arrow).

After immobilizing the dogs, ink marks were drawn on tape placed on the mask's external surface, in the approximate region centrally to the brain to be able to correlate the room laser isocenter to the radiation machine imaging isocenter. Three CT markers (Suremark® CT labels CT-23, The Suremark Company, Simi Valley, CA) were placed where the ink marks intersected on the dorsal and both lateral aspects of the thermoplastic mask.

A Varian Clinac 21EX 6MV linear accelerator (Varian Medical Systems, Palo Alto, CA) with an OBI system (On-Board Imager Advanced Imaging, Varian Medical Systems, Palo Alto, CA), and equipped with a 4DOF couch with 1-mm shift capability in the three translational directions and a minimum of 0.1° yaw rotation capability. The OBI system has two parts: the x-ray source is positioned at 270° and the receptor at 90° relative to the gantry angle (Figure 2.2).

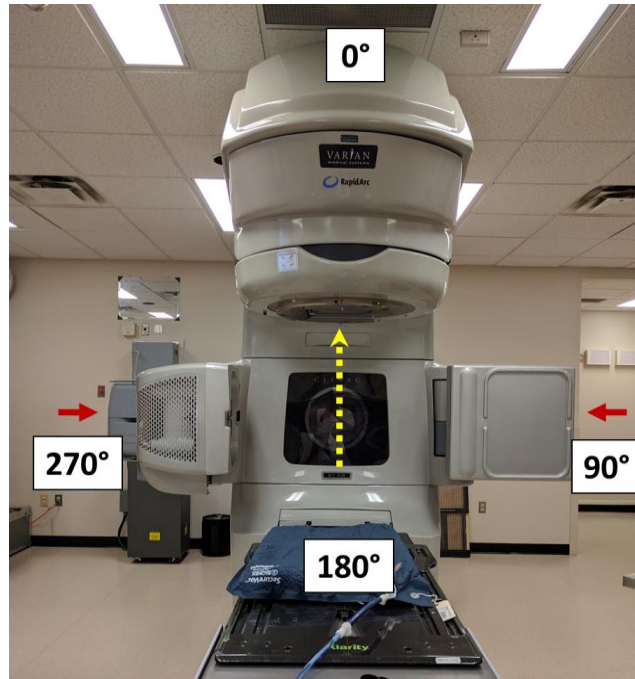


Figure 2.2. The OBI system (solid arrows) and the gantry (dotted arrow) of a Varian Clinac 21EX 6MV linear accelerator.

Using the OBI system, the reference CBCT scan was acquired sequentially after the immobilization procedure. The CBCT scan parameters were 100kV, 150mAs, 2mm slice thickness, 0.49mm x 0.49mm pixel size, and a gantry rotation from 22° to 178° counter-clockwise or clockwise. The reference orthogonal kV images were also acquired, and the imaging parameters were 70-80kVp and 200mA, with gantry angles of 0° and 270°.

2.3.3. Quality assurance

The gantry, collimator and yaw couch angles are verified every month. The tolerance for this quality assurance procedure is 1mm and 0.1° in yaw rotation, which is in accordance to the VRTOG standards (LaDue and Klein 2001).

The linear accelerator, the OBI system, and the couch shift accuracy are tested daily at the Veterinary Medical Centre. An ion chamber-based device (CheckMate-2, Sun Nuclear Corporation, FL) is used for the linear accelerator output quality assurance, and a deviation of 2% is considered to be an acceptable tolerance. The OBI system and couch shifts are tested using kV radiographs on a phantom with embedded markers. The markers are aligned using image registration with the kV images to the isocenter, and the couch is moved. A 1-mm difference between the gantry isocenter and the collimator isocenter is considered acceptable for this quality assurance procedure.

2.3.4. Test set-ups and image guidance

In order to perform unbiased CBCT image matching, the lead markers were obscured using OsiriX v.3.9.3 software. Not only the lead marker, but also the area around the lead marker was also obscured using the software. Dorsoventral and lateral DRR views were reconstructed from the edited reference CBCT, using the Eclipse™ software (Varian Medical Systems, Palo Alto, CA).

Using the immobilization system and the room lasers, each subject was repositioned 45 times simulating a clinical set-up in a canine patient treated with radiation therapy. The set-ups were made by an American College of Veterinary Radiology board-certified radiation oncologist (Monique Mayer) and a graduate student (Celina Morimoto).

Three modalities for image guidance were used: orthogonal kV radiographs, orthogonal MV radiographs, or CBCT. For each experimental group, 15 set-ups were made alternating between modalities. Using ARIA software (Varian Medical Systems, Palo Alto, CA), the test kV radiographs and test MV radiographs were registered to the

reference DRRs, while the test CBCT was matched to the reference CBCT (Figure 2.3). All test set-ups verified with image guidance were manually performed by a certified radiation therapist with five years of experience in veterinary radiation oncology (Rachel Bloomfield).

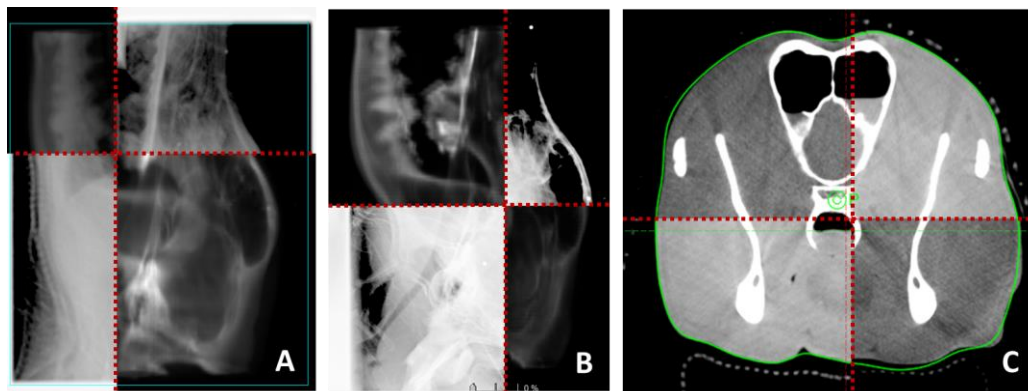


Figure 2.3. Image matching for patient position correction. A: a lateral view MV radiograph matched with the reference DRR. B: a lateral view kV radiograph matched with the reference DRR. C: transverse view CBCT image matched with the reference CBCT.

The couch shifts in the lateral, longitudinal, and vertical directions, and yaw rotations after image guidance were calculated by the ARIA software (Varian Medical Systems, Palo Alto, CA) and applied. No further imaging for couch correction was performed after couch shifts were made. Shifts larger than 5mm or yaw rotations larger than 2 degrees were considered unacceptable. For every unacceptable displacement, the dog was re-positioned, and image guidance performed again. Although pitch was not possible to correct, this rotation was assessed by comparing the displacement between

the palatine portion of the maxillary bone and the external occipital protuberance. If the vertical distance between those anatomical landmarks were $\geq 3\text{mm}$, the set-up was considered unacceptable.

After the image-guided couch correction was performed, one dorsoventral and one lateral orthogonal kV image was taken.

2.3.5. Data collection

The lead marker positions were measured relatively to the kV imaging isocenter. The set-up error (3D displacement) was defined as the difference between the reference kV marker positions and the marker positions on the kV radiographs when the dogs were repositioned using an immobilization device, with or without couch corrections following image guidance.

The lead markers were measured in the three translational directions, in which the lateral (left to right) and longitudinal (caudal to rostral) vectors were measured from the dorsoventral view, acquired at a 270° gantry angle. The vertical vector (ventral to dorsal) was measured from the lateral radiograph view, with the gantry at 0° .

For the kV-DRR match experimental group, the radiographs taken to match the dogs' positions to the reference DRR were also used to measure the accuracy of the positioning device without image guidance.

One single observer (Celina Morimoto) performed all the measurements ($n = 5,400$) using the ARIA Offline Review software (Varian Medical Systems, Palo Alto, CA), and an interobserver variability comparison was performed to detect a possible subjectivity in measuring the markers on the radiographs. A second observer (Monique

Mayer) measured 180 data points using the same software. One pair of radiographs from each dog was compared to the measurements from the first observer. The two observers analyzed the data independently. The data were recorded using Microsoft Office Excel 2016 software (Microsoft Corporation, Redmond, WA).

2.3.6. Statistical analysis

All data analyses were performed by an analytic epidemiologist (Cheryl Waldner). The data was stratified by experimental group (no image guidance, MV-, kV-, or CBCT-image-guided correction), set-up (set-up 1-15), subject (dogs 1 to 6), lead marker location (1 to 5). The 3D displacement was calculated using the following formula (AAPM Task Group 42, 1995):

$$\sqrt{(x_A - x_B)^2 + (y_A - y_B)^2 + (z_A - z_B)^2} \dots\dots\dots(2.1)$$

where (x_A, y_A, z_A) represent the coordinates of the fiducial markers on the reference images, and (x_B, y_B, z_B) , the coordinates on the test set-up images (AAPM Task Group 68, 2005).

The 3D displacement difference among the four experimental groups were estimated performing pairwise comparisons using mixed-effects linear regression with random effects to account for repeated measures for each subject, individual set-ups and lead markers (STATA/SE version 14 for Windows, StataCorp, College Station, TX).

Using a similar mixed-effects logistic regression model, we evaluated if when the set-up without image guidance was greater than 1mm, the set-up after kV-guided correction was also more likely to be greater than 1mm. The same was performed for

when no image guidance was greater than 1mm, 2mm and 3mm, with the effect on the set-up after kV-guided correction being greater than 1mm, 2mm, and 3mm.

The interobserver variability analysis consisted on using Lin's concordance coefficient (STATA/SE version 14 for Windows, StataCorp, College Station, TX).

For all analyses, differences with $p < 0.05$ were considered statistically significant.

2.4. Results

2.4.1. 3D displacement before and after image guidance

The 95th percentile of the mean 3D displacement for each experimental group was 4.2mm, 2.8mm, 2.6mm, and 3.6mm for pre-image guidance, MV-, kV-, and CBCT-image guidance, respectively.

The analysis of the mean relative to zero showed that there was a large displacement of 1.3mm to the ventral direction in the CBCT-image guidance experimental group. The remaining experimental groups showed no displacements larger than 1mm in any direction based on the mean relative to zero. Table 2.1 summarizes the results of this experimental study. The statistical analysis showed that there was no difference between the mean 3D displacement before image correction and after MV-image guidance ($p=0.31$). For all other comparisons, the mean 3D displacement was statistically different ($p < 0.01$).

2.4.2. 3D displacement and the residual set-up error

The residual set-up error was affected by the 3D displacement prior to image-guided couch corrections. If the 3D displacement before image-guided correction was

>2mm, the post-kV residual set-up error was more likely to be >2mm (OR=2.38, 95%CI 1.17-4.82, p=0.016). Furthermore, if the 3D displacement before image-guided correction was >3mm, the post-kV residual set-up error was also more likely to be >2mm (OR=3.74, 95%CI 1.38-10.15, p=0.01).

2.4.3. Interobserver variability

The interobserver variability for measuring the lead marker positions to the image isocenter was very small (Lin's concordance coefficient 1.000; SE <0.001, n=177). The average difference was <0.001 with a SD=0.004.

Table 2.1. Translational and 3D displacements (millimeters) prior to image-guided set-up and after MV-, kV-, and CBCT-image-guided couch corrections in six cadaver dogs (n = 90 set-ups for each condition)

Condition		L-R ^a	V-D ^b	C-R ^c	3D displacement
Before image guidance	Mean Relative to Zero ^d	0.1	-0.4	-0.6	-
	Absolute Mean ^e	0.7	0.9	1.1	1.7
	95%CI ^f	0.6, 0.8	0.6, 1.1	0.8, 1.3	1.4, 2.0
	95th Percentile	2.0	2.7	2.8	4.2
MV	Mean Relative to Zero ^d	0.6	0.7	0.4	-
	Absolute Mean ^e	0.8	0.9	1.0	1.7
	95%CI ^f	0.7, 0.9	0.6, 1.1	0.7, 1.2	1.4, 2.0
	95th Percentile	1.8	1.9	2.1	2.8
kV	Mean Relative to Zero ^d	0.3	0	0	-
	Absolute Mean ^e	0.6	0.7	0.9	1.5
	95%CI ^f	0.6, 0.7	0.5, 1.0	0.6, 1.1	1.2, 1.8
	95th Percentile	1.6	2.0	2.2	2.6
CBCT	Mean Relative to Zero ^d	0.7	-1.3	0.6	-
	Absolute Mean ^e	0.8	1.5	1.0	2.2
	95%CI ^f	0.7, 0.9	1.2, 1.7	0.7, 1.2	1.9, 2.5
	95th Percentile	1.9	3.2	2.1	3.6

^aLeft-Right vector

^bVentral-Dorsal vector

^cCaudal-Rostral vector

^dFor calculation of the mean relative to zero, displacements to left, ventral and caudal directions were assigned a negative value.

^eThe absolute mean was reported so that errors in opposite directions did not cancel each other out.

^f95% Confidence Interval, calculated using the mixed effects linear regression model

2.5. Discussion

This study results supports our initial hypothesis that the repositioning accuracy based on the 95th percentile of the mean 3D displacement is improved after image guidance, compared to when image guidance is not used. However, we did not expect to find that CBCT guidance would not provide an advantage in repositioning accuracy compared to the other two modalities tested.

Overall, the residual set-up error was higher than expected for the three image guidance technologies tested. To the authors' knowledge, this is the first veterinary study that reported the set-up error after couch corrections are applied based on image guidance with MV, kV or CBCT.

Among the different methods for set-up margin calculation published in the literature, we chose to report the 95th percentile of the 3D displacement. The mean 3D displacement itself would not represent a margin number as it does not represent the width of error probability distribution. Knowing that the data in this study did not follow a normal distribution, the use of the 95th percentile supports selection of a PTV margin generated directly from this experimental model, and it would guarantee that the GTV is encompassed in 95% of the patient set-ups (AAPM Task Group 68, 2005).

Although the methods of measuring set-up error differ in the literature, other studies have reported the set-up positioning accuracy without image guidance (Kent et al. 2009; Hansen et al. 2015; Dieterich et al. 2015). Using different immobilization systems, the range of the 95th percentile reported in all studies were between 3.5 to 6.4mm. Our 95th percentile of the 3D displacement of 4.2mm before image guidance falls within the interval reported in the veterinary literature.

The current study relied on laser alignment of ink marks on the thermoplastic mask. The authors noted that there was some variability when the screws attaching the mask to the carbon fiber board were tightened, and this could contribute to a larger error in patient positioning prior to image guidance.

Considering the numerous sources of uncertainties that can happen during patient set-up and repositioning, it is unlikely that a zero error would be achieved. Some of the uncertainties were described in Chapter 1, and include: localization accuracy of CT and CBCT, accuracy of image registration, mechanical uncertainties of the equipment, variations in patient positioning, uncertainties in target delineation, and others.

Two human phantom studies have used a similar methodology to evaluate set-up errors. For CT-guided repositioning, a mean 3D displacement \pm SD of 1.33 ± 0.64 mm was used to calculate an error of less than 2.4mm in 95% of the individual treatments (Lutz, Winston, and Malleki 1988). For CBCT-guided repositioning, a mean 3D displacement \pm SD of 1.34 ± 0.33 mm has been reported (Chang et al. 2007). Using the same methodology as reported by Lutz *et al.* (1988), the 95th percentile of CBCT-guided repositioning in a human head phantom was 1.9mm.

Considering that both phantom studies were not limited by couch shifts, the error is expected to be smaller than the current study. Differently from the phantom studies cited, the image guidance in our experimental study was solely based on bony image registration, without using the lead markers for repositioning of the dogs. Larger errors would be expected when anatomical targets are used for image registration.

Opposing our initial hypothesis, MV and kV image-guided repositioning resulted in a smaller error compared to CBCT image guidance. Although CBCT allows verification of

all three rotation planes, the use of a 4DOF limits patient correction in pitch and roll rotations. Therefore, the advantage of detecting rotations on a CBCT scan is not used to its full extent.

In addition, we found a large ventral displacement after CBCT-guided correction. This study design eliminates the possibility of having a systematic error introduced by the difference in CBCT isocenter. The reference CBCT and kV images were taken sequentially, without moving the dogs from the table. Even with differences in the CBCT and the kV image isocenters, the setup error measured for CBCT guidance would not be influenced by those differences. This is because the reference CBCT was compared with the verification CBCT to correct position, and the reference kV radiograph was compared with the kV image for lead marker position measurement. Furthermore, we hypothesized that by using sagittal and dorsal reconstructions on CBCT, only a single plane of the scan is taken into consideration. For this reason, the fact that the overlay in the skull anatomy was not possible using the sagittal and dorsal planes of CBCT reconstruction, a systematic error during manual image registration was possibly introduced.

Because of the nature of orthogonal kV and MV radiographs acquisition, the two modalities are able to capture the full anatomy of the bones, and this could have led to a better repositioning accuracy when these 2D imaging techniques are used for intracranial targets. Based on our findings, MV and kV radiographs can be considered as adequate repositioning image modalities, even when highly conformal targets are necessary for high dose hypofractionated radiation therapy.

In our data analysis, it was found that if the 3D displacement prior to image guidance was small, the residual set-up error was also small. Therefore, the results

support that the positioning error prior to image verification should be minimized using immobilization systems that provide the best repositioning repeatability.

The current PTV margin used at the Western College of Veterinary Medicine, University of Saskatchewan, is 1mm around the GTV with CBCT image guidance prior to every fraction to be delivered. Increasing the PTV margin could result in simultaneously increased risk of side effects to normal tissues, but also an increase in tumor control probability by reducing the chance of a geographical miss of the target. A larger isotropic PTV margin is being considered by the authors.

The outcomes reported using high dose hypofractionated radiation therapy have been similar to conventionally fractionated protocols. The PTV margins reported for SRS or SRT have been 0mm (Kelsey, Gieger, and Nolan 2018; Mariani et al. 2013) and 1-2mm (Griffin et al. 2014), respectively.

Although mechanical uncertainties and human errors may vary between institutions, other sources of uncertainties may not be possible to extinguish, such as couch shift limitation to correct errors smaller than 1mm, localization accuracy of CT and CBCT, and image registration accuracy. The methodology of the current study did not capture errors from CT image transfer to the radiation machine unit or imaging isocenter to radiation isocenter differences. These should be taken into consideration when choosing the PTV margins to account for possible uncertainties in radiation treatment delivery.

The error introduced by CT image isocenter transfer to the radiation isocenter was not quantified in our study, and it should be added separately when margins are selected for radiotherapy planning. The reason CBCT scans were used as a reference image was

because reference kV radiographs needed to measure marker position could be acquired at the same time without moving the dog from the treatment table.

Some limitations of the current study are related to manual image registrations performed by a single observer. On the other hand, the limitation of having one individual measuring the lead marker positions was proven to be eliminated, as the interobserver variability was shown to be very small.

Another limitation is that correction of pitch and roll rotations could lead to an increase in repositioning accuracy if a 6DOF couch was used. Furthermore, a couch with a submillimeter shift capability may contribute to a smaller residual set-up error for all imaging modalities for patient position verification.

2.6. Conclusion

This study confirmed that image guidance decreases the probability of errors in patient set-up for radiation targets in the intracranial region. When highly conformal PTV margins are required, such as in SRT or SRS treatments, image guidance prior to every radiation fraction should be performed to reduce the chance of set-up errors. However, this study has shown that the residual set-up errors were larger than expected, and not within the submillimeter range as hypothesized previous studies (Harmon, Van Ufflen, and LaRue 2009; Dieterich et al. 2015). Further studies exploring the use of more accurate immobilization devices should be conducted aiming to reduce the residual set-up error in the current linear accelerators available for veterinary patients.

Under the conditions of this experimental design using a 4DOF couch with 1-mm shift capability, image guidance with kV or MV resulted in a better repositioning accuracy

compared to CBCT-image guidance. The 3D displacement found in this experimental design favors the use of MV and kV over CBCT for stereotactic radiosurgery protocols and stereotactic radiation treatments, where match is performed based only on the bony anatomy for the intracranial region.

Transition from research project 1 to research project 2

The study described in Chapter 2 found that the 95th percentile of the 3D displacement that represents the residual set-up errors using image guidance with MV radiographs, kV radiographs, or CBCT, in combination with the VMC device was larger than originally expected, ranging from 2.6 to 3.6mm. The 95th percentile of the 3D displacement set-up error without image guidance in our initial experiment was within the range reported in the literature.

Based on set-up errors reported with different immobilization devices available for the canine head region, the HRD has shown to provide a repositioning accuracy of 1.9mm. For this reason, we decided to evaluate the effect of the HRD and the residual set-up error after MV- or CBCT-image-guidance described in Chapter 3.

3. CHAPTER THREE: RESIDUAL SET-UP ERROR FOR CANINE BRAIN RADIATION THERAPY AFTER MV AND CBCT ONLINE CORRECTION USING A HEAD-REPOSITIONER SYSTEM FOR IMMOBILIZATION

This chapter will be submitted for publication. The copyright of this chapter will belong to the journal it will be published in.

3.1. Abstract

In our first study on residual set-up error we found that if the set-up error prior to image guidance is small, the residual set-up error was also small. The goal of this second study was to quantify the residual set-up error using the HRD immobilization system (Charney et al., 2009) after MV-, and CBCT-image guidance and couch shift corrections are performed for the canine patients treated with radiotherapy in the head region. Six dogs were positioned 24 times using the HRD. The residual set-up error was determined by measuring the position of the implanted five lead markers based on kV orthogonal radiographs. The 95th percentiles of the 3D displacements after online MV, and CBCT-guided correction were 2.1mm, and 2.9mm, respectively, and 2.8mm for the immobilization device with no image guidance procedures. There was a statistically significant difference in the set-up error ($p=0.019$) between the VMC device without image-guidance and the HRD without image-guidance. This is possibly attributable to the inclusion of all upper molar teeth in the HRD's bite block.

3.2. Introduction

Clinical studies have reported different PTV margins used to encompass set-up errors in canine brain tumor patients. Although statistical significance between different studies cannot be analyzed, good outcomes were reported in studies with canine brain tumors treated with different irradiation protocols (Keyerleber et al. 2013; Griffin et al. 2014; Kelsey, Gieger, and Nolan 2018). Therefore, as the PTV margins reported for SRS and SRT were 0 and 1-2mm (Griffin et al. 2014; Kelsey, Gieger, and Nolan 2018), respectively. It is possible that tumor volumes may be missed in clinical treatments using SRS or SRT, but acceptable outcomes have been achieved with this newer technology despite the possibility of a target missed.

A veterinary study describing the head-repositioning device (HRD) designed by Charney *et al.* (2009) has found that the mean 3D displacement and its 95th percentile without any type of image-guided technology was very small, measuring 0.9mm and 1.9mm, respectively (Mayer et al. 2010). Furthermore, a better repositioning capability has also been reported in another veterinary study when a larger portion of the maxilla is immobilized (Nemoto et al. 2015).

Our previous finding supports that the accuracy on patient position prior to image guidance affects the residual set-up error after couch corrections. Furthermore, considering that a small error is achieved when the HRD is used (Mayer et al. 2010), we aimed to evaluate the effect of image guidance based on MV- and CBCT-image guidance using the HRD to immobilize the patients. For this study, we hypothesized that there would be no difference between the 3D set-up errors for the head region when the HRD is used alone or in combination with MV or CBCT image-guided couch corrections.

3.3. Materials and Methods

3.3.1. Subject preparation

Six dog cadavers (median weight 20.0kg, range 18.6-27.6kg) with a mesaticephalic skull conformation were used in this experimental study. The study protocol was approved by the University of Saskatchewan's Animal Research Ethics Board (Animal Use Protocol Number 014CatA2017). The subject preparation was similar to the methodology described in Chapter 2.

3.3.2. Immobilization and reference image acquisition

The dogs were immobilized in sternal recumbency using the HRD (Charney et al. 2009). This immobilization device has a full-body wooden board that is not indexed to the treatment table, a plastic maxillary plate with drilled holes that allow the maxillary teeth to protrude through, and a moldable bite block (VP Mix Putty Regular Set, Henry Schein, Melville, NY) is placed on the top surface of the maxillary plate (Figure 3.1). The maxillary plate length covered all the teeth, and the bite block encompassed all upper incisors, canines and premolar teeth.

Medical tape was placed on the skin, dorsal to the nasal bone region to hold the maxilla in the maxillary plate. In order to reduce possible pitch rotation, a rigid Styrofoam pillow was placed in the ventral neck area.

Pen marks on masking tape were placed on the wooden board where the room lasers aligned during the reference set-up. In this experimental design, the HRD's Z-plate was only used for laser alignment. The Z-plate consists of two lateral acrylic plastic plates and a removable top plate that connects the two lateral parts. The side plates are fastened

with plastic wing screws to the wooden board in a reproducible manner. The room lasers were aligned with one of the Z-plate's left and right 1mm-grooves. When a difference in vertical and/or horizontal laser alignment between the two lateral surfaces of the Z-plate were seen during the test set-ups, the difference was split between both sides. The top plate was aligned with the field light from the radiation machine's gantry.

Three CT markers (Suremark® CT labels CT-23, The Suremark Company, Simi Valley, CA) were placed where the room lasers crossed on both lateral surfaces, and the field light simultaneously overlapped the top surface of the Z-plate (Figure 3.1).

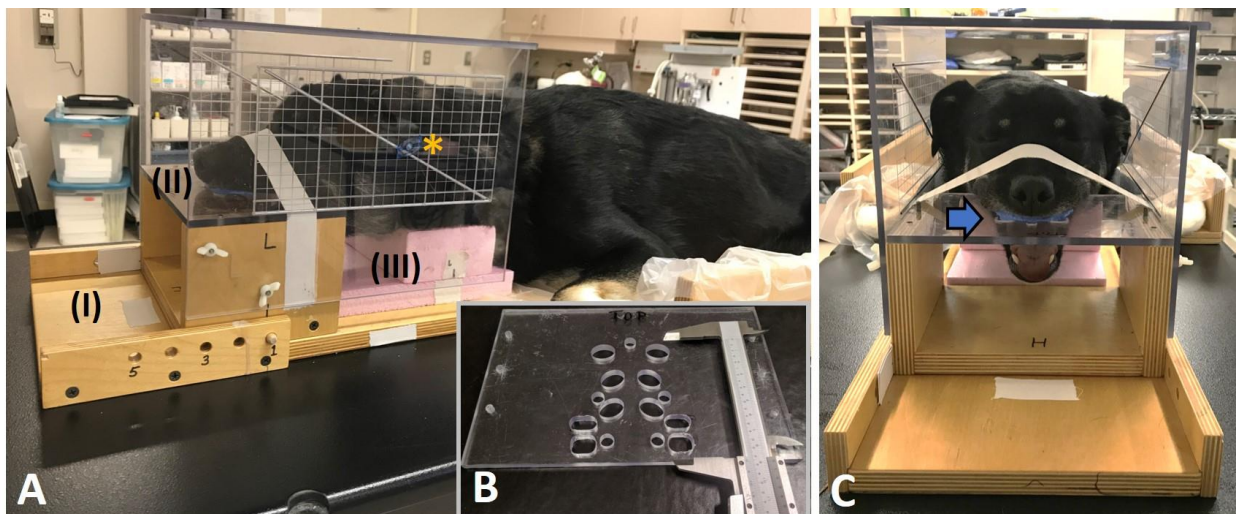


Figure 3.1. A: One CT marker on the surface of the Z-plate (asterisk); the head-repositioning device has a full-body wooden board (I), a plastic maxillary plate (II), and a rigid Styrofoam pillow (III). B: the plastic maxillary plate showing the drilled holes that allow the maxillary teeth to protrude through. C: the moldable bite block (arrow).

The same linear accelerator, OBI system, radiation treatment couch, and scan parameters described in Chapter 2 were used in this experiment. A reference CBCT scan

and reference orthogonal kV radiographs were acquired immediately after immobilizing each subject.

3.3.3. Quality assurance

The quality assurance protocol and the system accuracy tolerance were kept the same during the studies described in Chapters 2 and 3.

3.3.4. Test set-ups and image guidance

The lead markers were also obscured in this experimental design using OsiriX v.3.9.3 software. Not only the lead marker, but also the area around the lead marker was obscured using the software. The dorsoventral and lateral DRR images were generated from the lead marker-obscured reference CBCT scan using Eclipse™ software (Varian Medical Systems, Palo Alto, CA).

Each subject was repositioned 24 times using the HRD and room lasers. All set-ups were made by the same personnel from the experiment described in Chapter 2. All image registrations with MV and reference DRR (n = 12 set-ups) and CBCT with the reference CBCT (n = 12 set-ups) were performed by the same radiation therapist as in the study described in Chapter 2. The lateral, longitudinal, and vertical couch shifts, and yaw rotations were calculated and applied using ARIA software (Varian Medical Systems, Palo Alto, CA). If the couch shifts were not within the acceptable tolerance of 5mm in translational vectors or 2 degrees in yaw rotation, the set-up was re-done, and image guidance was repeated.

For all test set-ups, the kV images were acquired prior to the image-guided correction in both experimental groups to evaluate the positioning accuracy of the dogs without image guidance, using only the positioning device.

After every image-guided couch correction, a pair of orthogonal kV radiographs was taken to measure the residual set-up error after image guidance with MV or CBCT, using the HRD for patient immobilization. Each pair of x-ray image consisted of one dorsoventral and one lateral view of the skull.

3.3.5. Data collection

The set-up error was calculated using the difference between the lead markers on the reference kV to the image isocenter and the markers on each test set-up to the isocenter. The same methodology for data collection was used from the study described in Chapter 2.

One single observer (Celina Morimoto) performed all the data collection of 1,435 measurements. One pair of kV images acquired after MV image-guided couch correction had failed to transfer to the ARIA system, and the lead markers distance to the image isocenter could not be measured.

3.3.6. Statistical analysis

Data analyses were made by an analytic epidemiologist (Cheryl Waldner). The data was stratified by experimental group (no image guidance, MV- or CBCT-image-guided correction), subject (dogs 7 to 12), set-up (1 to 12), and lead marker location (1 to 5). The 3D displacement was calculated using the square root of the sum square

differences in the three translational vectors (x, y, z), applying the square root of x, y, and z square sum.

The 3D displacements difference between the three experimental groups were compared using mixed-effects linear regression, and the random effects to account for repeated measures for each dog, individual set-ups and lead markers (STATA/SE version 14 for Windows, StataCorp, College Station, TX).

For the comparison between the HRD (Chapter 3) and the VMC device (Chapter 2), a mixed-effects linear regression was made, and the random effects to account for repeated measures for each dog (1-12), set-ups (1-15) and lead markers (1-5).

For all analyses, differences with $p < 0.05$ were considered statistically significant.

3.4. Results

3.4.1. 3D displacement before and after image guidance

The 95th percentile of the mean 3D displacement for each experimental group was 2.8mm, 2.1mm, and 2.9mm for pre-image guidance, MV-, and CBCT-image guidance, respectively.

The analysis of the mean relative to zero showed that there was a large ventral displacement of 1.1mm in the CBCT group. The lateral, ventrodorsal, and cranio-caudal for the other groups were smaller than 1mm. This is consistent to what has been found in the experiment described in Chapter 2. Table 3.1 summarizes the results of this experimental study.

There was no statistically significant difference between the mean 3D displacement for MV-image guidance and the use of the HRD alone ($p=0.53$). The

difference between the mean 3D displacement for all the other comparisons were statistically significant ($p < 0.01$).

Table 3.1. Translational and 3D displacements (millimeters) prior to image-guided set-up and after MV-, and CBCT-image-guided couch correction in six cadaver dogs (n = 72 set-ups for each condition).					
Condition		L-R ^a	V-D ^b	C-R ^c	3D displacement
Before image guidance	Mean Relative to Zero ^d	0.5	0	0.1	-
	Absolute Mean ^e	0.7	0.5	0.6	1.2
	95%CI ^f	0.3, 1.1	0.4, 0.5	0.5, 0.6	0.9, 1.5
	95 th Percentile	2.7	1.3	1.4	2.8
MV	Mean Relative to Zero ^d	0.3	0.6	0.2	-
	Absolute Mean ^e	0.5	0.7	0.7	1.2
	95%CI ^f	0.1, 0.9	0.6, 0.7	0.6, 0.8	0.9, 1.5
	95 th Percentile	1.0	1.6	1.6	2.1
CBCT	Mean Relative to Zero ^d	0.4	-1.1	0.9	-
	Absolute Mean ^e	0.6	1.1	1.2	1.9
	95%CI ^f	0.2, 1.0	1.1, 1.2	1.1, 1.3	1.6, 2.2
	95 th Percentile	1.5	2.2	2.3	2.9

^aLeft-Right coordinate

^bVentral-Dorsal coordinate

^cCaudal-Rostral coordinate

^dFor calculation of the mean relative to zero, displacements to left, ventral and caudal directions were assigned a negative value.

^eThe absolute mean was reported so that errors in opposite directions did not cancel each other out.

^f95% Confidence Interval, calculated using the mixed effects linear regression model

3.4.2. Comparison between two different immobilization devices

The results obtained in the experiment using the VMC device were compared to the results using the HRD. Our data show that the repositioning accuracy is significantly better with the HRD than the VMC device ($p=0.019$). When MV image guidance is used, the repositioning accuracy was shown to be statistically better with the HRD than the VMC device ($p=0.027$). On the other hand, there was no difference between the HRD and the VMC device when CBCT image guidance was used ($p=0.231$). The data is summarized in Table 3.2 below:

Condition	VMC device Mean (95% CI)	HRD Mean (95% CI)	p-value
No imaging	1.7 (1.4, 2.0)	1.2 (0.9, 1.5)	0.019
MV	1.7 (1.4, 2.0)	1.2 (0.9, 1.5)	0.027
CBCT	2.2 (1.9, 2.5)	1.9 (1.6, 2.2)	0.231

3.5. Discussion

Comparing the use of immobilization devices without the use of image-guided techniques in the two studies described in Chapters 2 and 3, the repositioning accuracy was shown to be significantly better when the HRD was used than when current VMC device used ($p=0.019$). Identical methodologies were used in both studies involving the

same personnel. Although different dog individuals were used in the two experiments, the exclusion and inclusion criteria were similar.

It is likely that the most impactful differences between the two immobilization systems were the increased maxilla stability and the less mobile laser alignment method used in the HRD. The thermoplastic bite block in the maxillary plate from the VMC device did not cover the incisors to all premolar teeth while the moldable bite block from the HRD did. Furthermore, the HRD had larger holes in which the bite block and the subject's teeth protruded, whereas the other device had only three 6mm holes to lock the thermoplastic material into the maxillary plate.

The ink marks drawn on the thermoplastic mask dorsal and lateral surfaces aligned to the room lasers in the previously studied immobilization system (VMC device) contributed to some variability in positioning depending on the degree that the screws were tightened to the carbon fiber board. On the other hand, the authors noticed that the HRD had a subjectively better reproducibility alignment between the room laser and the Z-plate grooves.

Another study has compared two immobilization devices with different types maxillary plates (Nemoto et al. 2015). The maxillary plate that supported the canines and all four premolar teeth had a significantly better repositioning accuracy compared to the maxillary plate that supported the canine teeth alone. The better repositioning accuracy is likely due to a greater stability of the maxilla when the premolar teeth are included in the maxillary plate.

Although methodologies for measuring the 3D displacement differed, three other studies have reported the 95th percentile ranging from 3.5mm to 6.4mm using different

immobilization systems (Kent et al. 2009; Hansen et al. 2015; Dieterich et al. 2015). The 95th percentile in this current study achieved a smaller value (2.8mm) compared to the range reported in the literature.

A similar study design in this same institution (Mayer et al. 2010) reported a mean 3D displacement without the use of image guidance which was smaller than our current experiment, 0.9mm and 1.2mm, respectively. The 95th percentile in the previous study was also smaller, measuring 1.9mm versus our current value of 2.8mm. Although both studies used similar methodologies, the current study had a larger sample size of 6 dogs and 144 set-ups whereas the previous study had used 3 dogs and 45 set-ups. For this reason, the current study would be a better representation of the HRD's repositioning accuracy.

The mean 3D displacement of the HRD alone was not statistically different from the mean 3D displacement when this immobilization device was used in combination with MV guidance. However, the width of the error distribution probability quantified by the 95th percentile value was smaller when MV guidance was used compared to when the use of the HRD alone.

On the other hand, CBCT-guided corrections did not reduce the 95th percentile or the mean 3D displacement compared to when the HRD was used alone. It was expected that the use of image guidance would decrease the width of error probability distribution, as it happened to MV-guided corrections compared to when the immobilization device was used alone. One reason that might explain this result is that CBCT relies on reconstruction of the sagittal and the dorsal planes. Therefore, it is not possible to visualize the full anatomy of the skull in one single slice (Figure 3.2) as in MV radiographs

(Figure 3.3), and this could result in increased errors after CBCT-image-guided couch shifts.

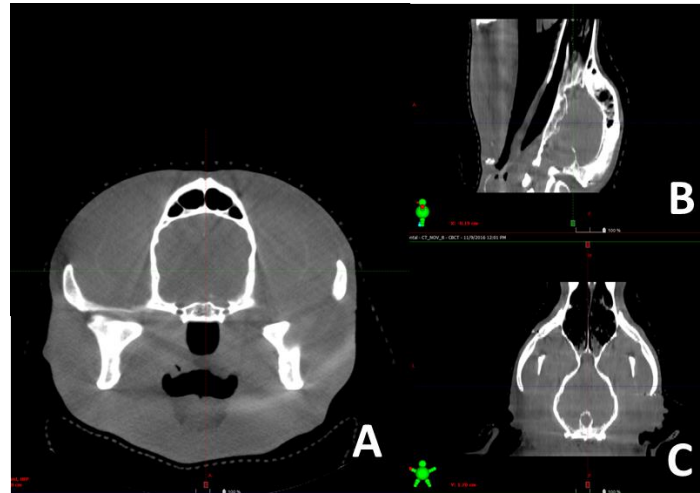


Figure 3.2. CBCT images showing the original acquisition plane (A), sagittal plane reconstruction (B), dorsal plane reconstruction (C). Note that each slice does not display the full anatomy of the skull.

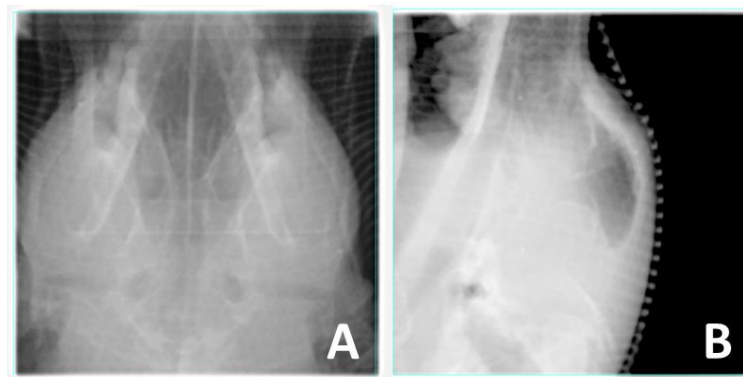


Figure 3.3. MV radiographs showing the dorsoventral (A) and the lateral (B) views displaying the full anatomy of the skull.

We compared the use of the two different immobilization devices from our experiments followed by MV- or CBCT-guided couch corrections. We did not assess kV-image-guided corrections in this study to reduce the total number of set-ups necessary to achieve an adequate sample size. Furthermore, MV radiographs are more common to other veterinary radiation facilities that are not equipped with an OBI. The OBI system is capable of both kV and CBCT imaging.

The repositioning accuracy was statistically higher when MV-image guidance and the HRD were used in combination, compared to the use of MV and the VMC device. It was found that there was no significant difference between the two types of immobilization devices when CBCT-guided corrections were performed. This is likely because a larger error was introduced by CBCT guidance procedure in both experiments, and the advantage of having a more accurate immobilization device did not overcome the error introduced by CBCT-image guidance.

3.6. Conclusions

According to the results of this study, on the contrary to what has been hypothesized in the veterinary literature (LaRue and Custis 2014; Dieterich et al. 2015), the use of CBCT image guidance prior to radiation therapy delivery did not provide the best positioning accuracy for intracranial targets in veterinary patients when a 4DOF is used.

The comparison between this study and our previous experiment has found that the use of an accurate immobilization system is needed to minimize residual set-up error. Based on the results of this study, the best repositioning accuracy can be achieved when

the HRD is used in combination with MV image-guided couch corrections. This finding is limited to an EPID with an online registration software, and results cannot be applied to MV port films with image registrations performed without the use of a software. Limitations of using CBCT-guided couch corrections should be considered when this technology is used in the head region.

4. CHAPTER FOUR: GENERAL DISCUSSION

Recent publications have discussed the validity of the linear-quadratic (LQ) model in predicting tumor cell kill for SRS or SRT (Garau 2017; Brown, Brenner, and Carlson 2013; Brown, Carlson, and Brenner 2014). This model has been accepted to be an adequate representation of the tumor response to conventional radiation protocols (Hall and Giaccia 2012).

In the LQ model, two variables that influence cell killing by radiation are combined, and they depend on the dose of radiation given. One variable, α , is proportional to a linear model, and β is proportional to a quadratic distribution. The combination of the two variables is named α/β ratio, and it results in a cell survival curve that is continuously bending (Hall and Giaccia 2012) because cell killing is exponentially increased with dose.

Another mathematical model that uses the α/β ratio is the biologically effective dose (BED). The BED formula is used in clinical radiation therapy to compare the biological effect of different fractionation protocols. The use of IMRT techniques in SRS and SRT have allowed delivery of higher doses to the tumors, with minimal increase of occurrence of acute side effects in the peritumoral normal tissues. One possible theory that could explain the successful outcomes in SRS and SRT treatment is that higher BED can be achieved with higher doses per fraction. As a consequence, the tumor control probability is also expected to increase (Brown, Carlson, and Brenner 2014).

While widely accepted for predicting tumor response to conventionally fractionated radiation protocols, one limitation of using the LQ model to predict cell killing by SRS and SRT is that the data is based on *in vitro* studies in tumor cells, and it only considers that cell death is caused by DNA strand breaks. It is hypothesized that other mechanisms of

cell death may occur with SRT and SRS. Furthermore, the fractional doses considered in the development of the LQ model were below the doses used in SRT and SRS treatments.

When previous studies that reported outcomes in canine brain meningiomas irradiated with different techniques (conventional or SRS/SRT) are evaluated (Keyerleber et al. 2013; Griffin et al. 2014; Kelsey, Gieger, and Nolan 2018), the importance of targeting the entire GTV can be questioned, as these studies report prolonged survival while using PTV margins that were too small to ensure a high probability of GTV coverage. Our experiment described in chapter 3 has found that even when the HRD is used, which has shown highly accurate repositioning capability, a PTV margin of at least 2.1mm would be required to encompass the residual set-up errors in 95% of the individual treatments. That is, the use of PTV margins equal to or smaller than 2mm would likely be resulting in a geographical miss of the tumor volumes.

A possible explanation for the good outcomes even if the GTV was not fully encompassed include the “New Radiobiology” hypothesis, which suggests that the tumor microenvironment also plays a role in radiation-induced cell death (Garau 2017). This theory supports that targeting the entire GTV with high radiation doses might not be necessary when SRS or SRT protocols are delivered.

“New Radiobiology” Hypothesis

It has been hypothesized by Brown *et al.* (2014) that the tumor response to high dose hypofractionated radiation therapy can be explained by two main mechanisms

(Brown, Carlson, and Brenner 2014), beyond the classical factors that are known to affect tumor response to irradiation.

Enhanced antitumor immunity

Anti-tumor immune response may be induced by SRS/SRT, leading to death of tumor cells. Studies in melanoma have found that irradiation of the tumor at one site contributes to an antitumor immunologic rejection of a metastatic lesion at a distant site. This phenomenon has been called the *abscopal effect* (Garau 2017), where *ab-* means “position”, and *-scopos* refers to “mark or target for shooting”. In a study by Lee *et al.* (2009), wild-type mice with implanted B16 melanoma cells were irradiated with a single fraction of 20Gy (Lee *et al.* 2009). The authors found that T cells were increased in the tumor area and in the lymphoid tissues 1 to 2 weeks post radiation. In nude mice (T-cell deficient), the tumor was radioresistant. This study concludes that high single dose of radiation in B16 melanoma tumors elicits T CD8⁺-mediated cell response.

Another study has found that radiation enhances the antigenicity of carcinoma models, and it is greater for SRT treatments when compared to SRS, with 8Gy per fraction protocols delivered in 3 fractions being the most effective (Dewan *et al.* 2009).

Secondary effects from injured vasculature

The higher doses per fraction used in SRS and SRT may affect vasculature, leading to death of tumor cells. The secondary effects of vascular damage can occur due to endothelial cell apoptosis. The effect of reoxygenation of hypoxic regions is very important for tumor response to conventional fractionated radiation treatments. Park *et*

al. (2012) reported that the tumor vasculature of regions irradiated with conventional fractionated protocols appear to remain structurally intact and functional during the early period after irradiation, and this gradually decreases in the last treatments (Park et al. 2012). However, the authors found that vascular damage post irradiation seems to be proportional to the amount of radiation delivered in single doses, with more severe effects when the doses used in SRS and SRT treatments are used, such as reduction in blood perfusion.

How should errors and margins be added?

Although in practice they are added linearly, the internal margins and set-up margins should be added quadratically because those variables are based on probabilities and they have random components (ICRU Report 91, 2017). Adding those margins in quadrature would represent the width of probability distributions (van Herk 2004).

If all sources of uncertainties described in section *1.5 Sources of Uncertainties* are added linearly, the errors in patient set-up would be in the order of dozens of millimeters, or a few centimeters. However, using a large margin to account for all possible uncertainties during treatment planning and delivery is also not the best solution because of risk of damage to normal tissues surrounding the tumor (ICRU Report 91, 2017).

In contrast, the use of zero margins around the tumor volume would likely result in a geographical miss, and this could result in partial tumor underdosage (van Herk 2004). The author also states that it is impossible to completely eliminate all geometrical errors

due to the multiple variables that can contribute to treatment uncertainties, and they cannot be accounted without the use of margins (van Herk 2004).

We have used the 95th percentile to report the adequate margin to account for the set-up errors because it accounts for the width of error probability distribution of this data set. By using the 95th percentile method, some factors that contribute to errors in patient set-up were accounted for, such as localization accuracy of CT/CBCT and mechanical uncertainties of the equipment related to couch shift precision in translational directions and inability to correct roll and pitch rotations.

We were not able to quantify other sources of uncertainties, such as accuracy of image registration, other mechanical uncertainties (e.g. difference in isocenter between room lasers, the OBI and the radiation machine gantry), and uncertainties in target delineation.

Some variabilities in tumor delineation can be reduced by implementing peer-reviewed and collaborative approaches with other specialties to achieve an individualized treatment plan for each patient, and to reduce the risk of a geographical miss. The creation of a contouring atlas, and workshops to generate contouring consensus would aid in decreasing intraobserver and interobserver variabilities.

5. CHAPTER FIVE: CONCLUSIONS AND FUTURE DIRECTIONS

The two experiments described in this work were limited by the set-up ability to identify and correct errors in only one (yaw) of the three possible rotations, with a 1-mm couch shift capability in the translational directions.

Using the 4DOF couch of this facility's linear accelerator, we found that there was no advantage of CBCT over 2D imaging verification technologies (kV and MV radiographs) for correcting rotational errors. We concluded that CBCT should not be the first choice for image-based set-up correction in the head region. Instead, if kV radiographs are available for patient set-up correction, it should be preferably used over CBCT scans for the canine head region radiation therapy. More studies are necessary to evaluate the effect on the residual set-up error after kV image guidance in a 6DOF couch equipped with submillimeter shift capability.

We have shown that the use of the HRD can decrease set-up error with or without image guidance. Therefore, we recommend using this system, with maxillary plates that could ensure the immobilization of all upper molar teeth in canine patients receiving radiation treatment in the head region.

Survival times achieved in canine brain meningiomas treated with SRT or SRS treatments have been reported to be similar to conventional fractionated radiation therapy. Although we found that a margin of more than 2mm is necessary to guarantee that the GTV would be encompassed in 95% of the patient set-ups using the HRD with image guidance, the results in the veterinary literature have reported good outcomes using margins less than or equal to 2mm (Griffin et al. 2014; Kelsey, Gieger, and Nolan 2018). Therefore, the need for targeting 100% of the GTV should be questioned when

SRS or SRT are used to treat intracranial tumors in dogs. On the other hand, it should also be considered that better outcomes might be achievable using a PTV of at least 2mm. Multiple plans from each patient should be individually evaluated, and if the normal tissue tolerance is met using a margin of 2mm or more, the larger margin should be applied to reduce the chance of a geographical miss and to decrease the chance of tumor recurrence.

REFERENCES

- AAPM Task Group 101. 2010. "Stereotactic Body Radiation Therapy." *Medical Physics* 37 (8):4078–4101. <https://doi.org/10.1118/1.3438081>.
- AAPM Task Group 42. 1995. "Stereotactic Radiosurgery."
- AAPM Task Group 68. 2005. "Intracranial Stereotactic Positioning Systems." *Medical Physics* 32 (7):2380–98. <https://doi.org/10.1118/1.1945347>.
- Bley, Carla Rohrer, Andrea Sumova, Malgorzata Roos, and Barbara Kaser-hotz. 2005. "Irradiation of Brain Tumors in Dogs with Neurologic Disease." *J Vet Intern Med* 19:849–54.
- Brown, J Martin, David J Brenner, and David J Carlson. 2013. "Dose Escalation, Not 'New Biology', Can Account for the Efficacy of Stereotactic Body Radiation Therapy with Non-Small Cell Lung Cancer." *Int J Radiation Oncology Biol Phys* 85 (5). Elsevier Inc.:1159–60. <https://doi.org/10.1016/j.ijrobp.2012.11.003>.
- Brown, J Martin, David J Carlson, and David J Brenner. 2014. "The Tumor Radiobiology of SRS and SBRT: Are More than the 5 Rs Involved?" *Int J Radiation Oncology Biol Phys* 88 (2). Elsevier Inc.:254–62. <https://doi.org/10.1016/j.ijrobp.2013.07.022>.
- Cattaneo, Giovanni Mauro, Michele Reni, Giovanna Rizzo, Pietro Castellone, Giovanni Luca Ceresoli, Cesare Cozzarini, Andrés José Maria Ferreri, Paolo Passoni, and Riccardo Calandrino. 2005. "Target Delineation in Post-Operative Radiotherapy of Brain Gliomas: Interobserver Variability and Impact of Image Registration of MR (Pre-Operative) Images on Treatment Planning CT Scans." *Radiotherapy and Oncology* 75:217–23. <https://doi.org/10.1016/j.radonc.2005.03.012>.
- Chang, Jenghwa, Kamil M. Yenice, Ashwatha Narayana, and Philip H. Gutin. 2007. "Accuracy and Feasibility of Cone-Beam Computed Tomography for Stereotactic Radiosurgery Setup." *Medical Physics* 34 (6):2077–84. <https://doi.org/10.1118/1.2731031>.
- Charney, Sarah, Wendell R. Lutz, Mary K. Klein, and Pamela D. Jones. 2009. "Evaluation of a Head-Repositioner and Z-Plate System for Improved Accuracy of Dose Delivery." *Veterinary Radiology and Ultrasound* 50 (3):323–29. <https://doi.org/10.1111/j.1740-8261.2009.01544.x>.

- Dewan, M Zahidunnabi, Ashley E Galloway, Noriko Kawashima, J Keith Dewyngaert, James S Babb, Silvia C Formenti, and Sandra Demaria. 2009. "Fractionated but Not Single-Dose Radiotherapy Induces an Immune-Mediated Abscopal Effect When Combined with Anti-CTLA-4 Antibody." *Clin Cancer Res* 15 (17):5379–89. <https://doi.org/10.1158/1078-0432.CCR-09-0265>.
- Dhillon, Amanpreet, Darby Erler, Ian Poon, Justin Lee, Danny Enepekides, Kevin Higgins, Lee Chin, and Irene Karam. 2017. "The Impact of Correcting for Translational and Rotational Errors Using the HexaPOD in Head and Neck Stereotactic Body Radiation Therapy Patients." *Journal of Medical Imaging and Radiation Sciences* 48:276–81.
- Dieterich, Sonja, Allison Zwingenberger, Katherine Hansen, Isabella Pfeiffer, Alain P. Théon, and Michael S. Kent. 2015. "Inter- and Intrafraction Motion for Stereotactic Radiosurgery in Dogs and Cats Using a Modified Brainlab Frameless Stereotactic Mask System." *Veterinary Radiology and Ultrasound* 56 (5):563–69. <https://doi.org/10.1111/vru.12271>.
- Dolera, M., L. Malfassi, C. Bianchi, N. Carrara, S. Finesso, S. Marcarini, G. Mazza, S. Pavesi, M. Sala, and G. Urso. 2017. "Frameless Stereotactic Radiotherapy Alone and Combined with Temozolomide for Presumed Canine Gliomas." *Veterinary and Comparative Oncology*, 1–12. <https://doi.org/10.1111/vco.12316>.
- Fu, Lei, Harold Perera, Xiao Ying, and Yan Yu. 2014. "Importance of CBCT Setup Verification for Optical-Guided Frameless Radiosurgery." *Journal of Applied Clinical Medical Physics* 15 (3):32–40. <https://doi.org/10.1120/jacmp.v15i3.4487>.
- Garau, Miquel Macia i. 2017. "Radiobiology of Stereotactic Body Radiation Therapy (SBRT)." *Reports of Practical Oncology and Radiotherapy* 22. Greater Poland Cancer Centre:86–95.
- Griffin, L. R., M. W. Nolan, L. E. Selmic, E. Randall, J. Custis, and S. LaRue. 2014. "Stereotactic Radiation Therapy for Treatment of Canine Intracranial Meningiomas." *Veterinary and Comparative Oncology* 14 (4):158–70. <https://doi.org/10.1111/vco.12129>.
- Guckenberger, Matthias, Kurt Baier, Iris Guenther, Anne Richter, Juergen Wilbert, Otto Sauer, Dirk Vordermark, and Michael Flentje. 2007. "Reliability of the Bony Anatomy in Image-Guided Stereotactic Radiotherapy of Brain Metastases." *International*

- Journal of Radiation Oncology Biology Physics* 69 (1):294–301.
<https://doi.org/10.1016/j.ijrobp.2007.05.030>.
- Haken, R. K. Ten, A. F. Thronton, H. M. Sandler, M. L. LaVigne, D. J. Quint, B. A. Fraass, M. L. Kessler, and D. L. McShan. 1992. “A Quantitative Assessment of the Addition of MRI to CT-Based, 3-D Treatment Planning of Brain Tumors.” *Radiotherapy and Oncology* 25:121–33.
- Hall, Eric J., and Amato J. Giaccia. 2012. *Radiobiology for the Radiologist*. Seventh Ed. Lippincott Williams & Wilkins.
- Hansen, Katherine S., Alan P. Théon, Sonja Dieterich, and Michael S. Kent. 2015. “Validation of an Indexed Radiotherapy Head Positioning Device for Use in Dogs and Cats.” *Veterinary Radiology and Ultrasound* 56 (4):448–55.
<https://doi.org/10.1111/vru.12257>.
- Harmon, Joseph, Derek Van Ufflen, and Susan LaRue. 2009. “Assessment of a Radiotherapy Patient Cranial Immobilization Device Using Daily On-Board Kilovoltage Imaging.” *Veterinary Radiology and Ultrasound* 50 (2):230–34.
<https://doi.org/10.1111/j.1740-8261.2009.01522.x>.
- Herk, Marcel van. 2004. “Errors and Margins in Radiotherapy.” *Seminars in Radiation Oncology* 14 (1):52–64. <https://doi.org/10.1053/j.semradonc.2003.10.003>.
- Herk, Marcel van, Peter Remeijer, Coen Rasch, and Joos V. Lebesque. 2000. “The Probability of Correct Target Dosage: Dose-Population Histograms for Deriving Treatment Margins in Radiotherapy.” *Int J Radiation Oncology Biol Phys* 47 (4):1121–35.
- Huang, Yimei, Bo Zhao, Indrin J Chetty, Stephen Brown, James Gordon, and Ning Wen. 2016. “Targeting Accuracy of Image-Guided Radiosurgery for Intracranial Lesions: A Comparison across Multiple Linear Accelerator Platforms.” *Technology in Cancer Research & Treatment* 15 (2):243–48. <https://doi.org/10.1177/1533034615574385>.
- ICRU Report 62. 1999. “Prescribing, Recording and Reporting Photon Beam Therapy (Supplement to ICRU Report 50).”
- ICRU Report 83. 2010. “Prescribing, Recording, and Reporting Photon-Beam Intensity-Modulated Radiation Therapy (IMRT).” Vol. 10. <https://doi.org/10.1093/jicru/ndq001>.
- ICRU Report 91. 2017. “Prescribing, Recording, and Reporting of Stereotactic

Treatments with Small Photon Beams.” Vol. 14.

- Jansen, Edwin P M, Luc G H Dewit, Marcel van Herk, and Harry Bartelink. 2000. “Target Volumes in Radiotherapy for High-Grade Malignant Glioma of the Brain.” *Radiotherapy and Oncology* 56:151–56. [https://doi.org/10.1016/S0167-8140\(00\)00216-4](https://doi.org/10.1016/S0167-8140(00)00216-4).
- Kelsey, Krista L, Tracy L Gieger, and Michael W Nolan. 2018. “Single Fraction Stereotactic Radiation Therapy (Stereotactic Radiosurgery) Is a Feasible Method for Treating Intracranial Meningiomas in Dogs.” *Veterinary Radiology and Ultrasound*, 1–7. <https://doi.org/10.1111/vru.12636>.
- Kent, Michael S., Ira K. Gordon, Ines Benavides, Paul Primas, and Jacque Young. 2009. “Assessment of the Accuracy and Precision of a Patient Immobilization Device for Radiation Therapy in Canine Head and Neck Tumors.” *Veterinary Radiology and Ultrasound* 50 (5):550–54. <https://doi.org/10.1111/j.1740-8261.2009.01583.x>.
- Keyerleber, M. A., M. C. McEntee, J. Farrelly, M. S. Thompson, P. V. Scrivani, and C. W. Dewey. 2013. “Three-Dimensional Conformal Radiation Therapy Alone or in Combination with Surgery for Treatment of Canine Intracranial Meningiomas.” *Veterinary and Comparative Oncology* 13 (4):385–97. <https://doi.org/10.1111/vco.12054>.
- Khan, Faiz M., and John P. Gibbons. 2014. *The Physics of Radiation Therapy*. Fifth Edit. Lippincott Williams & Wilkins.
- Kippenes, Hege, Patrick R. Gavin, Ronald D. Sande, Dennis Rogers, and Vaugh Sweet. 2000. “Comparison of the Accuracy of Positioning Devices for Radiation Therapy of Canine and Feline Head Tumors.” *Veterinary Radiology and Ultrasound* 41 (4):371–76.
- Kubicek, Lyndsay N., Songwon Seo, Richard J. Chappell, Robert Jeraj, and Lisa J. Forrest. 2012. “Helical Tomotherapy Setup Variations in Canine Nasal Tumor Patients Immobilized with a Bite Block.” *Veterinary Radiology and Ultrasound* 53 (4):474–81. <https://doi.org/10.1111/j.1740-8261.2012.01947.x>.
- LaDue, Tracy, and Mary Kay Klein. 2001. “Toxicity Criteria of the Veterinary Radiation Therapy Oncology Group.” *Veterinary Radiology and Ultrasound* 42 (5):475–76.
- LaRue, Susan M, and James T. Custis. 2014. “Advances in Veterinary Radiation Therapy:

- Targeting Tumors and Improving Patient Comfort.” *Vet Clin Small Anim* 44 (5). Elsevier Inc:909–23. <https://doi.org/10.1016/j.cvsm.2014.05.010>.
- Lee, Youjin, Sogyong L Auh, Yugang Wang, Byron Burnette, Yang Wang, Yuru Meng, Michael Beckett, et al. 2009. “Therapeutic Effects of Ablative Radiation on Local Tumor Require CD8+ T Cells: Changing Strategies for Cancer Treatment.” *Blood* 114 (3):589–96. <https://doi.org/10.1182/blood-2009-02-206870>.
- Lutz, Wendell, Ken Winston, and Nasser Malleki. 1988. “A System for Stereotactic Radiosurgery with a Linear Accelerator.” *International Journal of Radiation Oncology Biology Physics* 14:373–81.
- Mariani, C L, T A Schubert, R A House, M A Wong, A L Hopkins, H L Barnes Heller, R J Milner, et al. 2013. “Frameless Stereotactic Radiosurgery for the Treatment of Primary Intracranial Tumours in Dogs.” *Veterinary and Comparative Oncology* 13 (4):409–23. <https://doi.org/10.1111/vco.12056>.
- Masi, Laura, Franco Casamassima, Caterina Polli, Claudia Menichelli, Ivano Bonucci, and Carlo Cavedon. 2008. “Cone Beam CT Image Guidance for Intracranial Stereotactic Treatments: Comparison with a Frame Guided Set-Up.” *International Journal of Radiation Oncology Biology Physics* 71 (3):926–33. <https://doi.org/10.1016/j.ijrobp.2008.03.006>.
- Mayer, Monique N., Cheryl L. Waldner, Kirsten M. Elliot, and Narinder Sidhu. 2010. “Comparison of Interfractional Variation in Canine Head Position Using Palpation and a Head-Repositioning Device.” *Veterinary Radiology and Ultrasound* 51 (4):472–76. <https://doi.org/10.1111/j.1740-8261.2010.01672.x>.
- Meeks, Sanford L., Frank J. Bova, Thomas H. Wagner, John M. Buatti, William A. Friedman, and Kelly D. Foote. 2000. “Image Localization for Frameless Stereotactic Radiotherapy.” *International Journal of Radiation Oncology Biology Physics* 46 (5):1291–99. [https://doi.org/10.1016/S0360-3016\(99\)00536-2](https://doi.org/10.1016/S0360-3016(99)00536-2).
- Nemoto, Yuki, Takuya Maruo, Yasuhiro Fukuyama, Shinpei Kawarai, Takuo Shida, and Tomohiro Nakayama. 2015. “A Novel Support Device for Head Immobilization during Radiation Therapy That Is Applicable to Both Cats and Dogs.” *Veterinary Radiology and Ultrasound* 56 (6):680–86. <https://doi.org/10.1111/vru.12274>.
- Park, Heon Joo, Robert J Griffin, Susanta Hui, Seymour H Levitt, and Chang W Song.

2012. "Radiation-Induced Vascular Damage in Tumors: Implications of Vascular Damage in Ablative Hypofractionated Radiotherapy (SBRT and SRS)." *Radiation Research* 177 (3):311–27. <https://doi.org/10.1667/RR2773.1>.
- Peng, J., Y. Chen, C. Liu, D. Kahler, and J. Li. 2010. "Dosimetric Consequences of Rotational Setup Errors Using Direct Simulation in a Treatment Planning System for Fractionated Stereotactic Radiotherapy." *Medical Physics* 37 (6):61–71. <https://doi.org/10.1118/1.3468383>.
- Rohrer Bley, Carla, Hans Blattmann, Malgorzata Roos, Andrea Sumova, and Barbara Kaser-Hotz. 2003. "Assessment of a Radiotherapy Patient Immobilization Device Using Single Plane Port Radiographs and Remote Computed Tomography Scanner." *Veterinary Radiology and Ultrasound* 44 (4):470–75.
- Rosenman, Julian. 2001. "Incorporating Functional Imaging Information into Radiation Treatment." *Seminars in Radiation Oncology* 11 (1):83–92. <https://doi.org/10.1053/srao.2001.18155>.
- Watanabe, M., R. Tanaka, and N. Takeda. 1992. "Magnetic Resonance Imaging and Histopathology of Cerebral Gliomas." *Neuroradiology* 34:463–69. <https://doi.org/10.1007/BF00598951>.
- Weltens, Caroline, Johan Menten, Michel Feron, Erwin Bellon, Philippe Demaerel, Frederik Maes, Walter Van Den Bogaert, and Emmanuel van der Schueren. 2001. "Interobserver Variations in Gross Tumor Volume Delineation of Brain Tumors on Computed Tomography and Impact of Magnetic Resonance Imaging." *Radiotherapy and Oncology* 60:49–59. [https://doi.org/10.1016/S0167-8140\(01\)00371-1](https://doi.org/10.1016/S0167-8140(01)00371-1).
- Withrow, Stephen J., David M. Vail, and Rodney L. Page. 2013. *Small Animal Clinical Oncology. Withrow and MacEwen's Small Animal Clinical Oncology*. Fifth Edit. Elsevier.